Available online at www.sciencedirect.com

ScienceDirect

Nuclear Physics B 987 (2023) 116113

NUCLEAR PHYSICS B

www.elsevier.com/locate/nuclphysb

The strong coupling $g_{XJ/\psi\phi}$ of $X(4700) \to J/\psi\phi$ in the light-cone sum rules

Yiling Xie [a], Dazhuang He [a], Xuan Luo [b], Hao Sun [a,*,1]

[a] *Institute of Theoretical Physics, School of Physics, Dalian University of Technology, No. 2 Linggong Road, 116024, Dalian, Liaoning, People's Republic of China*

[b] *School of Physics and Optoelectronics Engineering, Anhui University, Hefei, Anhui, 230601, People's Republic of China*

Received 30 August 2022; received in revised form 29 January 2023; accepted 6 February 2023
Available online 8 February 2023
Editor: Tommy Ohlsson

Abstract

We assign the scalar tetraquark and the D-wave tetraquark state for $X(4700)$ and calculate the width of the decay $X(4700) \to J/\psi\phi$ within the framework of light-cone sum rules. The strong coupling $g_{XJ/\psi\phi}$ is obtained by considering the technique of soft-meson approximation. We also investigate the mass and the decay constant of $X(4700)$ in the framework of SVZ sum rules. Our prediction for the mass is in agreement with the experimental measurement. For the decay width of $X(4700) \to J/\psi\phi$, if we assigns $X(4700)$ as a scalar $cs\bar{c}\bar{s}$ tetraquark state, we obtain $\Gamma = (109^{+35}_{-24})$ MeV. On the contrary, if $X(4700)$ is assigned as a D-wave tetraquark state, we obtain $\Gamma = (17.1^{+6.2}_{-4.0})$ MeV which is much smaller than the scalar one.

Contents

* Corresponding author.
E-mail addresses: xieyl_9@mail.dlut.edu.cn (Y. Xie), dzhe@mail.dlut.edu.cn (D. He), xuanluo@ahu.edu.cn (X. Luo), haosun@dlut.edu.cn (H. Sun).

[1] Hao Sun is supported by the National Natural Science Foundation of China (Grant No. 12075043, No. 12147205).

https://doi.org/10.1016/j.nuclphysb.2023.116113

1. Introduction

In 2016, the LHCb Collaboration analyzed the $B^+ \to J/\psi\phi K^+$ decay with 3 fb^{-1} data of pp collision at $\sqrt{s} = 7$ and 8 TeV [1,2], confirmed there are four resonances in the $J/\psi\phi$ mass spectrum, i.e., $X(4140)$, $X(4274)$, $X(4500)$ and $X(4700)$. The spin parity number of $X(4140)$ and $X(4274)$ states are determined to be $J^{PC} = 1^{++}$ with 5.7σ and 5.8σ significance, respectively. The J^{PC} of $X(4500)$ and $X(4700)$ states are 0^{++} with 5.2σ and 4.9σ significance, respectively. Their masses and widths are [1]

$$\begin{aligned}
X(4140):&\mathrm{M} = 4146.5 \pm 4.5^{+4.5}_{-2.8} && \text{MeV},\\
&\Gamma = 83 \pm 21^{+21}_{-14} && \text{MeV},\\
X(4274):&\mathrm{M} = 4273.3 \pm 8.3^{+17.2}_{-3.6} && \text{MeV},\\
&\Gamma = 56 \pm 11^{+8}_{-11} && \text{MeV},\\
X(4500):&\mathrm{M} = 4506 \pm 11^{+12}_{-15} && \text{MeV},\\
&\Gamma = 92 \pm 21^{+21}_{-20} && \text{MeV},\\
X(4700):&\mathrm{M} = 4704 \pm 10^{+14}_{-24} && \text{MeV},\\
&\Gamma = 120 \pm 31^{+42}_{-33} && \text{MeV}.
\end{aligned} \tag{1}$$

So $X(4700)$, $X(4500)$, $X(4140)$ and $X(4274)$ could be an important fraction of exotic mesons, and their study is necessary. Because the mass spectrum and hidden-flavor decay widths of $X(4140)$ and $X(4274)$ have already been systematically calculated with sum rules [3] in other previous works. Therefore, what we need to concern are $X(4700)$, $X(4500)$. In this paper, we only consider the $X(4700)$.

Since these resonance-like peaks appear in the $J/\psi\phi$ invariant mass spectrum, and $J/\psi\phi$ contains a $c\bar{c}$ pair and a $s\bar{s}$ pair, which implies that these states may be charmonium. The predicted mass of $\chi_{c0}(6P)$ is about 4669 MeV in the screened potential (SP) model [4], which is very close to that of $X(4700)$. But its predicted total width is only about 16 MeV, too narrow to be comparable with $120 \pm 31^{+42}_{-33}$ MeV, the observed width of $X(4700)$. Such discrepancy makes

it difficult to understand the structure of $X(4700)$ in this way. In the constituent quark model, the authors in Refs. [5,6] calculated the quark-antiquark spectrum for $J^{PC} = 0^{++}$ channels, and showed that $X(4700)$ could appear as conventional charmonium states with quantum numbers 5^3P_0 since it lies in the predicted mass and width ranges for 5^3P_0. According to Non-Relativistic QCD (NRQCD) results, $X(4700)$ is also compatible with a charmonium $\chi_{c0}(4P)$ [7]. However, the higher charmonium states like $\chi_{cJ}(nP)$ would have numerous decay modes to open charm mesons, unfortunately there is no relevant mass spectrum appears in the $B \to D^{(*)}_{(s)}\bar{D}^{*}_{(s)}K$ decays. In addition, the coupling of the higher charmonium states to $J/\psi\phi$ and to $J/\psi\omega$ should be very similar, but the BaBar collaboration measured the $J/\psi\omega$ mass spectrum in $B^+ \to J/\psi\omega K^+$ decay and did not find any structures resembling the $J/\psi\phi$ mass peaks [1,2], which contradicts a charmonium interpretation for the $X(4700)$.

Though $X(4700)$ can't be a pure charmonium, it could be explained as a hybrid state, a charmonium state contains excited gluon fields. According to NRQCD, the mass of 0^{++} hybrid $1p_0(H_3)$ state is 4566 MeV which is close to the spectrum of $X(4700)$. However, the charmonium fraction of 0^{++} hybrid is very small. So it is difficult to understand $X(4700)$ observed in the $J/\psi\phi$ channel since J/ψ mainly contains $c\bar{c}$ pair.

Besides hybrid, charmonium state can also be mixed with a light hadron to form a bound states, called hadrocharmonium. Considering that $X(4700)$ is observed in the $J/\psi\phi$ spectrum, it could be a bound state of $J/\psi - \phi$ or $\Psi(2S) - \phi$. However, the $J/\psi - \phi$ potential was found too weak, in lattice QCD, to form a bound states [8]. Furthermore, the $\Psi(2S) - \phi$ bound state has already been assigned to $X(4274)$ [9] so that rules out the possibility that $X(4700)$ be a s-wave $\Psi(2S) - \phi$ bound state. Anyway, $X(4700)$ could be other hadrocharmonium states in specific regions of the parameter space. Such explanation may require different binding mechanisms [9].

To extrapolate the intrinsic structure of $X(4700)$, a myriad of theoretical studies has turned to the $cs\bar{c}\bar{s}$ tetraquark state.

It was suggested in Ref. [10,11] that $X(4700)$ can be assigned as the 2S excited $cs\bar{c}\bar{s}$ tetraquark state. $X(4700)$ could also be explained as the radial excitation tetraquark state, for instance, of the hidden charm tetraquarks with quark content $\frac{1}{\sqrt{6}}(u\bar{u} + d\bar{d} - 2s\bar{s})c\bar{c}$ in a diquark-antidiquark model [12], or the S-wave radial excited compact tetraquark states within the framework of the color flux-tube model with a multibody confinement potential [13]. In addition, $X(4700)$ could be assigned as an first radial excitation of $X(4350)$ tetraquark state through the color-magnetic interaction model [14], or a 2S radial excited compact tetraquark state with $J^{PC} = 0^{++}$ in the chiral quark model [15].

Quite apart from the above excited tetraquark states explanation for $X(4700)$, there are several others. For example, it has been considered as a 0^{++} axial-vector diquark-antidiquark bound states in the diquark model [16], or a compact tetraquark state with $IJ^P = 00^+$ in the framework of the quark delocalization color screening model [17]. In particular, it can also be treated as a D-wave $cs\bar{c}\bar{s}$ tetraquark states [18] or a ground tetraquark state [19] by using the sum rule approach develop by Shifman, Vainshtein and Zakharov (SVZ sum rules) [20].

Although the above theories have claimed the resonance peak in the $J/\psi\phi$ mass spectrum corresponds to the genuine resonance, there are other opinions [21]. In Ref. [22,23], the authors have investigated the open-charmed mesons, $J/\psi K^{*+}$, $\psi' K^+$, and $\psi'\phi$ re-scattering effects or threshold cusps in the process $B^+ \to J/\psi\phi K^+$, in which $X(4700)$ can be simulated by the $\psi'\phi$ re-scattering via the $\psi' K_1$ loops. Anyway, within the available experimental data, none of these theoretical interpretations can be completely accepted or excluded to the nature of $X(4700)$. At this point, the structure of $X(4700)$ is not yet fully settled.

As we mentioned, with the method of SVZ sum rules, $X(4700)$ has been investigated in Ref. [18] and Ref. [19] in which its mass is predicted. Because of the deficiency of hidden-charm decay width, we consider the hidden-charm decay channel in this article. In this paper, we follow the same assumption that $X(4700)$ is a D-wave tetraquark state and a groud tetraquark state simultaneously. We evaluate the mass of $X(4700)$ in SVZ sum rules. The results are compared with the prediction in Ref. [18,19], and with the values in PDG [24] to ensure the credibility of our calculation. We then extend to evaluate the decay constant of $X(4700)$, which is needed in the numerical calculation of the strong coupling $g_{XJ/\psi\phi}$. While calculating $g_{XJ/\psi\phi}$, the interpolating currents are still taken from Ref. [18,19], and the method of light-cone sum rules (LCSR) is used and the full technical details are presented, in particular, the technique of soft-meson approximation is considered. Based on these calculations, we finally obtain the decay width of $X(4700) \to J/\psi\phi$. Then we compare the results of two different structures. As a charmoniumlike state, the main decay mode of the X(4700) could be the open-charm decay channels. Although the scalar tetraquark assignment yields a large width when we compare it with the total width of $X(4700)$, but this conclusion still has it's limitations before we consider the open-charm channels. The plan to calculate the open-charmed decay has been progressing. The calculations of the open-flavor decay widths will be the subject of a subsequent paper, the full results will provide us with more information to give a more rational conclusion. Our present study can be regarded as a supplement to other previous works.

Our paper is organized as follows: In Section. 2 the strong coupling $g_{XJ/\psi\phi}$ will be derived with the approach of light-cone sum rules. And we also calculate the mass and decay constant of the $X(4700)$ state within two-point SVZ sum rules approach. The numerical results and discussions are shown in Section. 3. We reach our summary in Section. 4.

2. Calculation framework

2.1. The mass and the decay constant of $X(4700)$

To calculate the mass and the decay constant, we start from the two-point correlation function:

$$\Pi_{\mathrm{I}}^{\mathrm{SVZ}}(p) = i \int \mathrm{d}^4x e^{ipx} \langle 0|T\{J_{\mathrm{I}}^{X}(x) J_{\mathrm{I}}^{X\dagger}(0)\}|0\rangle \,, \tag{2}$$

where $\mathrm{I} = (1), (2)$ and $J_{(1)}^{X}$, $J_{(2)}^{X}$ are the currents interpolate the $X(4700)$ in two different structures. They are given by [18,19]

$$\begin{aligned} J_{(1)}^{X}(x) =& \varepsilon_{ijk}\varepsilon_{imn}[s_j^T(x)C\gamma_\mu\gamma_5 c_k(x)][\bar{s}_m(x)\gamma_5\gamma^\mu C\bar{c}_n^T(x)], \\ J_{(2)}^{X}(x) =& c_a^T(x)C\gamma_{\mu 1}[D_{\mu 3}D_{\mu 4}s_b(x)](\bar{c}_a(x)\gamma_{\mu 2}C s_b^T(x) + \bar{c}_b(x)\gamma_{\mu 2}C\bar{s}_a^T(x)) \\ & \times(g^{\mu 1\mu 3}g^{\mu 2\mu 4} + g^{\mu 1\mu 4}g^{\mu 2\mu 3} - g^{\mu 1\mu 2}g^{\mu 3\mu 4}/2) \end{aligned} \tag{3}$$

where a, b, i, j, k, m, n are the color indexes and C is the charge conjugation matrix.

We first calculate the correlation function in terms of the phenomenological expression by inserting in Eq. (2) with a complete set of hadronic states:

$$\Pi_{\mathrm{I}}^{\mathrm{SVZ,phen}}(p) = \frac{\langle 0|J_{\mathrm{I}}^{X}|X(p)\rangle \langle X(p)|J_{\mathrm{I}}^{X\dagger}|0\rangle}{m_{\mathrm{I},X}^2 - p^2} + \int_{s'}^{\infty} d\hat{s} \frac{\rho_I^{\mathrm{SVZ,phen}}(\hat{s})}{\hat{s} - p^2}, \tag{4}$$

where $\rho_{\rm I}^{\rm SVZ,phen}(\hat{s})$ stands for the contributions of the higher resonances and the continuum states. The subtraction terms are not shown because they will vanish after the Borel transformation. After performing polarization sum we can derive

$$\Pi_{\rm I}^{\rm SVZ,phen}(p) = \frac{m_{{\rm I},X}^2 f_{{\rm I},X}^2}{m_{{\rm I},X}^2 - p^2} + \int_{s'}^{\infty} d\hat{s} \frac{\rho_{\rm I}^{\rm SVZ,phen}(\hat{s})}{\hat{s} - p^2}. \tag{5}$$

As we can see, there is a pole appearing on the right-hand side of Eq. (5). The way of removing the pole is to perform the Borel transformation on Eq. (5), which yields

$$\Pi_{\rm I}^{\rm SVZ,phen}(M^2) = m_{{\rm I},X}^2 f_{{\rm I},X}^2 e^{-m_{{\rm I},X}^2/M^2} + \int_{s'}^{\infty} d\hat{s} \rho_{\rm I}^{\rm SVZ,phen}(\hat{s}) e^{-\hat{s}/M^2}. \tag{6}$$

Now we turn to consider the correlation function in the OPE side, after contracting the heavy and light quark in term of Wick Theorm, we obtain

$$\begin{aligned}\Pi_{(1)}^{\rm SVZ,OPE}(p) =& i \int {\rm d}^4x e^{ipx} \epsilon_{ijk}\epsilon_{imn}\epsilon_{i'j'k'}\epsilon_{i'm'n'} {\rm Tr}[\tilde{S}_s^{jj'}(x)\gamma_\mu\gamma_5 S_c^{kk'}(x)\gamma_5\gamma_\alpha] \\ & {\rm Tr}[S_s^{mm'}(-x)\gamma_5\gamma_\mu \tilde{S}_c^{nn'}(-x)\gamma_\alpha\gamma_5],\end{aligned} \tag{7}$$

and

$$\begin{aligned}&\Pi_{(2)}^{\rm SVZ,OPE}(p) = i \int {\rm d}^4x e^{ipx} \\ &{\rm Tr}[\gamma_{\mu 1}(\overrightarrow{D}_{\mu 3}\overrightarrow{D}_{\mu 4} S_s^{bb'}(x-y)\overleftarrow{D}_{\nu 3}\overleftarrow{D}_{\nu 4})\gamma_{\nu 1}\gamma_5 \tilde{S}_c^{aa'}(-x)]|_{y=0} \\ &({\rm Tr}[\gamma_{\mu 2}\tilde{S}_s^{bb'}(-x)\gamma_{\nu 2} S_c^{aa'}(-x)] + {\rm Tr}[\gamma_{\mu 2}\tilde{S}_s^{ba'}(-x)\gamma_{\nu 2} S_c^{ab'}(-x)] \\ &- {\rm Tr}[\gamma_{\mu 2}\tilde{S}_s^{ab'}(-x)\gamma_{\nu 2} S_c^{ba'}(-x)] \\ &+ {\rm Tr}[\gamma_{\mu 2}\tilde{S}_s^{aa'}(-x)\gamma_{\nu 2} S_c^{bb'}(-x)](g^{\mu 1\mu 3}g^{\mu 2\mu 4} + g^{\mu 1\mu 4}g^{\mu 2\mu 3} - g^{\mu 1\mu 2}g^{\mu 3\mu 4}/2) \\ &\times(g^{\nu 1\nu 3}g^{\nu 2\nu 4} + g^{\nu 1\nu 4}g^{\nu 2\nu 3} - g^{\nu 1\nu 2}g^{\nu 3\nu 4}/2),\end{aligned} \tag{8}$$

where

$$\tilde{S}_q^{ab}(x) = C S_q^{ab}(x) C. \tag{9}$$

For propagators of the u, d and s quarks in coordinate-space. An expression for propagators is as follows [30,31]:

$$\begin{aligned}S_{q,ab}(x) =& \frac{i\delta_{ab}\not{x}}{2\pi^2x^4} - \frac{\delta_{ab}m_q}{4\pi^2x^2} - \frac{\langle\bar{q}q\rangle}{12} - \frac{i}{32\pi^2}\frac{\lambda^n}{2}g_s G_{\mu\nu}^n \frac{1}{x^2}(\sigma^{\mu\nu}\not{x} + \not{x}\sigma^{\mu\nu}) \\ &+ \frac{i\delta_{ab}\not{x}m_q\langle\bar{q}q\rangle}{48} - \frac{\delta_{ab}\langle\bar{q}g_s\sigma Gq\rangle x^2}{192} + \frac{i\delta_{ab}x^2\not{x}m_q\langle\bar{q}g_s\sigma Gq\rangle}{1152} \\ &- \frac{i\delta_{ab}x^2\not{x}g_s^2\langle\bar{q}q\rangle^2}{7776} - \frac{\delta_{ab}x^4\langle\bar{q}q\rangle\langle g_s^2GG\rangle}{27648}.\end{aligned} \tag{10}$$

Notice the situation here is different from LCSR, where we do not encounter the light quark propagator expressed in the coordinate-space. We have to face divergences in the double integrals like

$$\int \frac{d^4x}{x^{2n}} \int\int \frac{d^4k_1 d^4k_2 e^{ipx - ik_1x - ik_2x}}{(k_1^2 - m_c^2)(k_2^2 - m_c^2)}. \tag{11}$$

As shown in Ref. [32], by using Fourier transformation

$$\frac{1}{\left(x^2\right)^n}=\int\frac{d^Dp}{(2\pi)^D}e^{-ip\cdot x}i(-1)^{n+1}2^{D-2n}\pi^{D/2}\frac{\Gamma(D/2-n)}{\Gamma(n)}\left(-\frac{1}{p^2}\right)^{D/2-n} \tag{12}$$

and perform dimension regulation [33] and extract the imaginary part of results, we can obtain the results without any divergences.

The correlation function $\Pi_{\mathrm{I}}^{\mathrm{SVZ,OPE}}(p)$ can be represented as the dispersion integral

$$\Pi_{\mathrm{I}}^{\mathrm{SVZ,OPE}}(p)=\int_{4m_c^2}^{\infty}\mathrm{d}\hat{s}\frac{\rho_{\mathrm{I}}^{\mathrm{SVZ,OPE}}(\hat{s})}{\hat{s}-p^2}, \tag{13}$$

where $\rho_{\mathrm{I}}^{\mathrm{SVZ,OPE}}(\hat{s})$ is the corresponding spectral density.

By performing the Borel transformation on $\Pi_{\mathrm{I}}^{\mathrm{SVZ,OPE}}(p)$ and adopting the quark-hadron duality, one can obtain

$$\begin{aligned}\Pi_{\mathrm{I}}^{SVZ,OPE}(M^2,\infty)&\equiv\int_{4m_c^2}^{\infty}\mathrm{d}\hat{s}\tilde{\rho}_{\mathrm{I}}^{\mathrm{SVZ,OPE}}(\hat{s})e^{-\hat{s}/M^2}\\&=m_{\mathrm{I},X}^2f_{\mathrm{I},X}^2e^{-m_{\mathrm{I},X}^2/M^2}+\int_{s_0}^{\infty}\rho_{\mathrm{I}}^{\mathrm{SVZ,phen}}(\hat{s})e^{-\hat{s}/M^2}.\end{aligned} \tag{14}$$

Then subtract the continuum contribution yields:

$$m_{\mathrm{I},X}^2f_{\mathrm{I},X}^2e^{-m_{\mathrm{I},X}^2/M^2}=\int_{4m_c^2}^{s_0}\mathrm{d}\hat{s}\rho_{\mathrm{I}}^{\mathrm{SVZ,OPE}}(\hat{s})e^{-\hat{s}/M^2} \tag{15}$$

The mass of the $X(4700)$ state can be evaluated from the sum rule

$$m_{\mathrm{I},X}^2=\frac{\int_{4m_c^2}^{s_0}\mathrm{d}\hat{s}\hat{s}\rho_{\mathrm{I}}^{\mathrm{SVZ,OPE}}(\hat{s})e^{-\hat{s}/M^2}}{\int_{4m_c^2}^{s_0}\mathrm{d}\hat{s}\rho_{\mathrm{I}}^{\mathrm{SVZ,OPE}}(\hat{s})e^{-\hat{s}/M^2}}, \tag{16}$$

where the spectral densities are provided in Appendix A.2.

2.2. The strong coupling $g_{XJ/\psi\phi}$ in the LCSR

Before starting to predict the width of $X(4700)\to J/\psi\phi$, we need to calculate the strong coupling $g_{XJ/\psi\phi}$, in the framework of QCD LCSR. Let's strat by defining the two-point correlation function:

$$\Pi_{\mathrm{I},\mu}^{\mathrm{LC}}(p+q,q)=i\int\mathrm{d}^4xe^{ipx}\langle\phi(q)|T\{J_\mu^{J/\psi}(x)J_{\mathrm{I}}^{X\dagger}(0)\}|0\rangle, \tag{17}$$

where p, q are the four-momentum for J/ψ and ϕ respectively. Therefore $X(4700)$ has four-momentum $p'=p+q$ according to the momentum conservation. $J_\mu^{J/\psi}$ is the interpolating current of J/ψ [25,26]

$$J_\mu^{J/\psi}(x) = \bar{c}_i(x)\gamma_\mu c_i(x) \tag{18}$$

where i is the color index.

Next we need to establish a relation between the correlation function $\Pi^{\rm LC}_{{\rm I},\mu}(p',q)$ and the strong coupling $g_{XJ/\psi\phi}$. For a general dispersion relation, we have

$$\Pi^{\rm LC}_{{\rm I},\mu}(p',q) = \frac{1}{\pi^2}\int\int \frac{ds_1 ds_2 {\rm Im}\Pi^{\rm LC}_{{\rm I},\mu}(s_1,s_2)}{(s_1-p^2)(s_2-p'^2)} + \cdots \tag{19}$$

where the subtraction terms and the single dispersion integrals are not shown, all of them will vanish after applying the double Borel transformation to Eq. (19). Inserting in Eq. (17) with two complete sets of hadronic states and using Eq. (19), we obtain the phenomenological expression of the correlation function noted by $\Pi^{\rm LC,phen}_{{\rm I},\mu}(p',q)$

$$\begin{aligned}\Pi^{\rm LC,phen}_{{\rm I},\mu}(p',q) =& \frac{\langle 0|J_\mu^{J/\psi}|J/\psi(p)\rangle\,\langle\phi(q)J/\psi(p)|X(p')\rangle\,\langle X(p')|J_{\rm I}^{X\dagger}|0\rangle}{(p'^2-m^2_{{\rm I},X})(p^2-m^2_{J/\psi})} \\ &+ \int_{s_1^{0\prime}}^{\infty}\int_{s_2^{0\prime}}^{\infty} \frac{ds_1 ds_2\ \rho^{\rm LC,phen}_{{\rm I},\mu}(s_1,s_2)}{(s_1-p^2)(s_2-p'^2)} + \int_{s_1^{0\prime}}^{\infty}\frac{ds_1\ \rho^{\rm LC,phen}_{{\rm I},1,\mu}(s_1)}{(s_1-p^2)} \\ &+ \int_{s_2^{0\prime}}^{\infty}\frac{ds_2\ \rho^{\rm LC,phen}_{{\rm I},2,\mu}(s_2)}{(s_2-p'^2)}.\end{aligned} \tag{20}$$

Here contributions of the higher resonances and the continuum states are denoted by $\rho^{\rm LC,phen}_{{\rm I},\mu}(s_1, s_2)$, $s_1^{0\prime}$ and $s_2^{0\prime}$ denote the lowest thresholds of continuum states. $\rho^{\rm phen}_{{\rm I},1,\mu}(s_1)$ and $\rho^{\rm phen}_{{\rm I},2,\mu}(s_2)$ are the additional contributions to make the double dispersion integral finite [27]. The strong coupling $g_{XJ/\psi\phi}$ is defined as an invariant constant parameterizing the hadronic matrix element

$$\langle\phi(q)J/\psi(p)|X(p')\rangle = g_{XJ/\psi\phi}[-(q\cdot p)(\varepsilon^*\cdot\varepsilon') + (q\cdot\varepsilon^*)(p\cdot\varepsilon')], \tag{21}$$

and the decay constants here are defined as:

$$\begin{aligned}\langle X(p')|J_I^{X\dagger}|0\rangle &= m_{I,X}\ f_{I,X}, \\ \langle 0|J_\mu^{J/\psi}|J/\psi(p)\rangle &= m_{J/\psi}\, f_{J/\psi}\,\varepsilon_\mu,\end{aligned} \tag{22}$$

where ε, ε' are the polarization vectors of the J/ψ and ϕ respectively, $m_{J/\psi(X)}$ and $f_{J/\psi(X)}$ are the mass and decay constants of $J/\psi(X(4700))$.

By inserting Eq. (21) and (22) back to Eq. (20), and performing the polarization sum, we can derive

$$\begin{aligned}\Pi^{\rm LC,phen}_{{\rm I},\mu}(p',q) &= \frac{m_{J/\psi}\, f_{J/\psi}\ m_{\rm I,X} f_{\rm I,X}\ g_{\rm XJ/\psi\phi}}{(p'^2-m^2_{\rm I,X})(p^2-m^2_{J/\psi})}[(p\cdot q)\,\epsilon'_\mu - (p\cdot\epsilon')\,q_\mu] + \cdots \\ &= \Pi^{\rm LC,phen}_{\rm I}(p',q)[(p\cdot q)\epsilon'_\mu - p\cdot\epsilon' q_\mu],\end{aligned} \tag{23}$$

where we choose the structure proportional to ϵ'_μ to work with. The relevant form can be written as

$$\Pi_{\rm I}^{\rm LC,phen}(p',q)=\frac{m_{J/\psi}m_{{\rm I},X}f_{J/\psi}f_{{\rm I},X}g_{XJ/\psi\phi}}{(p'^2-m_{{\rm I},X}^2)(p^2-m_{J/\psi}^2)}+\int_{s_1^{0\prime}}^{\infty}\int_{s_2^{0\prime}}^{\infty}\frac{{\rm d}s_1{\rm d}s_2\rho_{\rm I}^{\rm LC,phen}(s_1,s_2)}{(s_1-p^2)(s_2-p'^2)}+\cdots. \quad (24)$$

Applying the Borel transformations on variables p^2 and $p'^2=(p+q)^2$ to the correlation function yields

$$\begin{aligned}\mathcal{B}_{p^2}(M_1^2)\mathcal{B}_{p'^2}(M_2^2)\Pi_{\rm I}^{\rm LC,phen}(p',q)&=m_{J/\psi}m_{{\rm I},X}f_{J/\psi}f_{{\rm I},X}g_{XJ/\psi\phi}\exp[-\frac{m_{J/\psi}^2}{M_1^2}-\frac{m_{{\rm I},X}^2}{M_2^2}]\\&+\int_{s_1^{0\prime}}^{\infty}\int_{s_2^{0\prime}}^{\infty}{\rm d}s_1{\rm d}s_2\exp[-\frac{s_1}{M_1^2}-\frac{s_2}{M_2^2}]\rho_{\rm I}^{\rm LC,phen}(s_1,s_2).\end{aligned} \quad (25)$$

To proceed, we represent the OPE result for the correlation function in the form of the double dispersion integral

$$\Pi_{\rm I}^{\rm LC,OPE}(p',q)=\int_{s_1'}^{\infty}\int_{s_2'}^{\infty}\frac{ds_1ds_2\ \rho_{\rm I}^{\rm LC,OPE}(s_1,s_2)}{(s_1-p^2)(s_2-p'^2)}+\cdots \quad (26)$$

with the double spectral density

$$\rho_{\rm I}^{\rm LC,OPE}(s_1,s_2)=\frac{{\rm Im}\Pi_{\rm I}^{\rm LC,OPE}(s_1,s_2)}{\pi^2}. \quad (27)$$

By choosing the structure proportional to ϵ'_μ and performing the Borel transformations on variables p^2 and $p'^2=(p+q)^2$, we find out

$$\Pi_{\rm I}^{\rm LC,OPE}(M_1^2,M_2^2)=\int_{s_1'}^{\infty}\int_{s_2'}^{\infty}{\rm d}s_1{\rm d}s_2\exp[-\frac{s_1}{M_1^2}-\frac{s_2}{M_2^2}]\rho_{\rm I}^{\rm LC,OPE}(s_1,s_2). \quad (28)$$

Then we employ the quark-hadron duality: assume the integral of the hadronic spectral density $\rho_{\rm I}^{\rm h}(s_1,s_2)$ in the region $\{s_1\geq s_1^{0\prime},s_2\geq s_2^{0\prime}\}$ is equal to the integral of the OPE spectral density $\rho_{\rm I}^{\rm LC,OPE}(s_1,s_2)$ in a certain region of $\{s_1\geq s_1^0,s_2\geq s_2^0\}$

$$\begin{aligned}&\int_{s_1^{0\prime}}^{\infty}\int_{s_2^{0\prime}}^{\infty}{\rm d}s_1{\rm d}s_2\exp[-\frac{s_1}{M_1^2}-\frac{s_2}{M_2^2}]\rho_{\rm I}^{\rm LC,phen}(s_1,s_2)=\\&\int_{s_1^{0}}^{\infty}\int_{s_2^{0}}^{\infty}{\rm d}s_1{\rm d}s_2\exp[-\frac{s_1}{M_1^2}-\frac{s_2}{M_2^2}]\rho_{\rm I}^{\rm LC,OPE}(s_1,s_2).\end{aligned} \quad (29)$$

Equating the double dispersion (25) and (28), and substituting (29) to (25), the result of LCSR for the strong coupling reads:

$$g_{XJ/\psi\phi} = \frac{1}{m_{J/\psi} m_{\mathrm{I},X} f_{J/\psi} f_{\mathrm{I},X}} \exp[\frac{m_{J/\psi}^2}{M_1^2} + \frac{m_{\mathrm{I},X}^2}{M_2^2}] \times \int_{s_1'}^{s_1^0}\int_{s_2'}^{s_2^0} \mathrm{d}s_1 \mathrm{d}s_2 \exp[-\frac{s_1}{M_1^2} - \frac{s_2}{M_2^2}] \rho_{\mathrm{I}}^{\mathrm{LC,OPE}}(s_1, s_2). \tag{30}$$

Nevertheless, our situation differs from the standard one. From Eq. (17), we see that the interpolating currents of $X(4700)$ is located at the space-time point $x = 0$, and the interpolating current of J/ψ is located at the point x. Therefore by contracting the $\bar{c}$ and c quark fields, there remain two light quarks s and $\bar{s}$ sandwiched between the ϕ state and the vacuum states, i.e., $\langle\phi(q)|[\bar{s}(0)s(0)]|0\rangle$. We encounter the situation that the correlation function depends not on $\langle\phi(q)|[\bar{s}(x)s(0)]|0\rangle$ but $\langle\phi(q)|[\bar{s}(0)s(0)]|0\rangle$, so that the ϕ distribution amplitude disappears and reduces to normalization factor. Such situation is possible to appear in the kinematical limit $q \to 0$ which means $(p+q) = p$, and the correlation function depends only on one variable p^2. Here, following Ref. [27], we adopt the approach of soft-meson approximation, taking the limit $q \to 0$ and dealing with the double pole terms.

The approximation of $q \to 0$ simplifies the hadronic side of the sum rules, but leads to a more complicated expression on its hadronic representation. The ground state depends only on the variable p^2:

$$\Pi_{\mathrm{I}}^{\mathrm{LC,phen}}(p) = \frac{m_{J/\psi} m_{\mathrm{I},X} f_{J/\psi} f_{\mathrm{I},X}}{(p^2 - m_{\mathrm{I,X}}^2)^2} g_{XJ/\psi\phi} + \cdots, \tag{31}$$

where $m_{\mathrm{I}}^2 = \frac{m_{J/\psi}^2 + m_{\mathrm{I},X}^2}{2}$ and the Borel transformation on the variable p^2 applied to this correlation function yields [27]

$$\Pi_{\mathrm{I}}^{\mathrm{LC,phen}}(p', q) = \frac{1}{M^2}(m_{J/\psi} m_{\mathrm{I},X} f_{J/\psi} f_{\mathrm{I},X} g_{XJ/\psi\phi} + AM^2) e^{\frac{-m_{\mathrm{I}}^2}{M^2}} + C, \tag{32}$$

where the constant A incorporates all unsuppressed contributions, and C contains all exponentially suppressed contributions. To remove unsuppressed contributions, we perform the operator that the script in [28]

$$(1 - M^2 \frac{d}{dM^2}) M^2 e^{m_{\mathrm{I}}^2/M^2} \tag{33}$$

on both sides of the sum rules expression: the phenomenological side and the OPE side. So Eq. (30) becomes

$$g_{XJ/\psi\phi} = \frac{1}{m_{J/\psi} m_{\mathrm{I},X} f_{J/\psi} f_{\mathrm{I},X}} (1 - M^2 \frac{d}{dM^2}) M^2 \times \int_{\hat{s}_0}^{\hat{s}'} \mathrm{d}\hat{s} \exp[\frac{m_{J/\psi}^2}{2M^2} + \frac{m_{\mathrm{I},X}^2}{2M^2} - \frac{\hat{s}}{M^2}] \rho_{\mathrm{I}}^{\mathrm{OPE}}(\hat{s}). \tag{34}$$

Because of soft-meson approximation, the continuum state depends not on two variables s_1 and s_2 but one that relabel as $\hat{s}$.

2.3. OPE side calculation

We already know that $g_{XJ/\psi\phi}$ is related to the OPE part of the correlation function, so we are going to calculate it. According to the Wick Theorem, we can obtain

$$\begin{aligned}\langle\phi(q)|\,\mathrm{T}\{J_\mu^{J/\psi}(x)J_{(1)}^{\mathrm{X}\dagger}(0)\}\,|0\rangle &= \langle\phi(q)|\,[\,\bar{s}_\alpha^a(0)s_\beta^d(0)\,]\,|0\rangle\\ &\times[\,\gamma_5\tilde{S}_c^{ib}(x)\gamma_\mu\tilde{S}_c^{ie}(-x)\gamma_\nu\gamma_5\\ &-\gamma_\nu\gamma_5\tilde{S}_c^{ib}(x)\gamma_\mu\tilde{S}_c^{ie}(-x)\gamma_5\,]_{\alpha\beta},\end{aligned} \tag{35}$$

and

$$\begin{aligned}\langle\phi(q)|\,\mathrm{T}\{J_\mu^{J/\psi}(x)J_{(2)}^{\mathrm{X}\dagger}(0)\}\,|0\rangle &= \langle\phi(q)|\,[\,(\bar{s}^b\overleftarrow{D}_{\mu4}\overleftarrow{D}_{\mu3})_\alpha(0)s_\beta^b(0)\,]\,|0\rangle\\ &\times[\,\gamma_{\mu1}\tilde{S}_c^{ac}(x)\gamma_\nu\tilde{S}_c^{ac}(-x)\gamma_{\mu2}\,]_{\alpha\beta}\\ &+\langle\phi(q)|\,[\,(\bar{s}^b\overleftarrow{D}_{\mu4}\overleftarrow{D}_{\mu3})_\alpha(0)s_\beta^a(0)\,]\,|0\rangle\\ &\times[\,\gamma_{\mu1}\tilde{S}_c^{ac}(x)\gamma_\nu\tilde{S}_c^{bc}(-x)\gamma_{\mu2}\,]_{\alpha\beta}\,.\end{aligned} \tag{36}$$

Therefore, the correlation functions become

$$\begin{aligned}\Pi_{(1),\mu}^{\mathrm{OPE}}(p',q) &= i\int d^4x e^{ipx}\,\langle\phi(q)|\,\mathrm{T}\{J_\mu^{J/\psi}(x)J_{(1)}^{\mathrm{X}\dagger}(0)\}\,|0\rangle\\ &= i\int d^4x e^{ipx}\varepsilon_{ijk}\varepsilon_{imn}\,\langle\phi(q)|\,[\,\bar{s}_\alpha^j(0)s_\beta^m(0)\,]\,|0\rangle\\ &\quad\times[\,\gamma_\mu\gamma_5\tilde{S}_c^{kl}(x)\gamma_\nu\tilde{S}_c^{nl}(-x)\gamma_\nu\gamma_5\,]_{\alpha\beta},\end{aligned} \tag{37}$$

and

$$\begin{aligned}\Pi_{(2),\mu}^{\mathrm{OPE}}(p',q) &= i\int d^4x e^{ipx}\,\langle\phi(q)|\,\mathrm{T}\{J_\mu^{J/\psi}(x)J_{(2)}^{\mathrm{X}\dagger}(0)\}\,|0\rangle\\ &= i\int d^4x e^{ipx}\{\langle\phi(q)|\,[\,(\bar{s}^b(0)\overleftarrow{D}_{\mu4}\overleftarrow{D}_{\mu3})_\alpha s_\beta^b(0)\,]\,|0\rangle\\ &\times[\,\gamma_{\mu1}\tilde{S}_c^{ac}(x)\gamma_\nu\tilde{S}_c^{ac}(-x)\gamma_{\mu2}\,]_{\alpha\beta}\\ &+\langle\phi(q)|\,[\,(\bar{s}^b(0)\overleftarrow{D}_{\mu4}\overleftarrow{D}_{\mu3})_\alpha s_\beta^a(0)\,]\,|0\rangle\\ &\times[\,\gamma_{\mu1}\tilde{S}_c^{ac}(x)\gamma_\nu\tilde{S}_c^{bc}(-x)\gamma_{\mu2}\,]_{\alpha\beta}\},\end{aligned} \tag{38}$$

where we introduce the notation

$$\tilde{S}_q(x) = CS_q^T(x)C, \tag{39}$$

and $S_q(x)$ is the propagator of quark q. For the heavy quark propagator on the light-cone we employ its expression in terms of [20]

$$\begin{aligned}S_c^{ab}(x) = i\int\frac{d^4k}{(2\pi)^4}e^{-ikx}[\,&\frac{\delta_{ab}(\not{k}+m_c)}{k^2-m_c^2}-\frac{g_sG_{ab}^{\alpha\beta}}{4}\frac{\sigma_{\alpha\beta}(\not{k}+m_c)+(\not{k}+m_c)\sigma_{\alpha\beta}}{(k^2-m_c^2)^2}]\\ &+\frac{g_sD_\alpha G_{\beta\lambda}^n t_{ij}^n(f^{\lambda\beta\alpha}+f^{\lambda\alpha\beta})}{3(k^2-m_c^2)^4}-\frac{g_s^2(t^at^b)_{ij}G_{\alpha\beta}^aG_{\mu\nu}^b(f^{\alpha\beta\mu\nu}+f^{\alpha\mu\beta\nu}+f^{\alpha\mu\nu\beta})}{4(k^2-m_c^2)^5},\end{aligned} \tag{40}$$

with

$$
\begin{aligned}
f^{\lambda\alpha\beta} &= (\not{k}+m_c)\gamma_\lambda(\not{k}+m_c)\gamma_\alpha(\not{k}+m_c)\gamma_\beta(\not{k}+m_c),\\
f^{\alpha\beta\mu\nu} &= (\not{k}+m_c)\gamma_\alpha(\not{k}+m_c)\gamma_\beta(\not{k}+m_c)\\
&\quad \gamma_\mu(\not{k}+m_c)\gamma_\nu(\not{k}+m_c),
\end{aligned}
\tag{41}
$$

here we use the shorthand notation

$$
G^{\mu\nu}_{ab} \equiv G^{\mu\nu}_i t^i_{ab}, \quad i = 1, 2, \cdots, 8. \tag{42}
$$

It is convenient to perform the summation over the color indices by performing the replacement

$$
\bar{s}^d_\alpha(0)s^{d'}_\beta(0) = \frac{1}{3}\delta_{dd'}\bar{s}_\alpha(0)s_\beta(0), \tag{43}
$$

and using the expansion

$$
\bar{s}_\alpha(0)s_\beta(0) \equiv \frac{1}{4}\Gamma^a_{\alpha\beta}\bar{s}(0)\Gamma^a s(0), \tag{44}
$$

where the sum runs over the Dirac structures a

$$
\Gamma^a = 1, \gamma_5, \gamma_\mu, i\gamma_5\gamma_\mu, \frac{\sigma_{\mu\nu}}{\sqrt{2}}. \tag{45}
$$

Substituting the summation Eq. (43) and the expansion Eq. (44) into Eq. (37) and Eq. (38), we obtain

$$
\begin{aligned}
\Pi_{(1),\mu}(p',q) &= i\int d^4x e^{ipx}\,\langle\phi(q)|T\{J^{J/\psi}_\mu(x)J^{X^\dagger}_{(1)}(0)\}|0\rangle\\
&= i\int d^4x e^{ipx}\varepsilon_{ijk}\varepsilon_{imn}\,\langle\phi(q)|[\bar{s}^j(0)\Gamma^a s^m(0)]|0\rangle\\
&\times \mathrm{Tr}[\gamma_\mu\gamma_5\tilde{S}^{kl}_c(x)\gamma_\nu\tilde{S}^{nl}_c(-x)\gamma_\nu\gamma_5\Gamma^a],
\end{aligned}
\tag{46}
$$

and

$$
\begin{aligned}
\Pi_{(2),\mu}(p',q) &= i\int d^4x e^{ipx}\,\langle\phi(q)|T\{J^{J/\psi}_\mu(x)J^{X^\dagger}_{(2)}(0)\}|0\rangle\\
&= i\int d^4x e^{ipx}\{\langle\phi(q)|[(\bar{s}^b(0)\overleftarrow{D}_{\mu4}\overleftarrow{D}_{\mu3})\Gamma^e s^b(0)]|0\rangle\\
&\times \mathrm{Tr}[\gamma_{\mu1}\tilde{S}^{ac}_c(x)\gamma_\nu\tilde{S}^{ac}_c(-x)\gamma_{\mu2}]\\
&+ \langle\phi(q)|[(\bar{s}^b(0)\overleftarrow{D}_{\mu4}\overleftarrow{D}_{\mu3})\Gamma^e s^a(0)]|0\rangle\\
&\times \mathrm{Tr}[\gamma_{\mu1}\tilde{S}^{ac}_c(x)\gamma_\nu\tilde{S}^{bc}_c(-x)\gamma_{\mu2}]\}.
\end{aligned}
\tag{47}
$$

The Feynman diagram of $\Pi_{(1),\mu}(p',q)$ is shown in Fig. 1 and the Feynman diagrams of $\Pi_{(2),\mu}(p',q)$ is shown in Fig. 2. Fig. 1 corresponds to the leading order and next-leading order contribution of $\Pi_{(1),\mu}(p',q)$. Fig. 2 corresponds to the leading order contribution of $\Pi_{(2),\mu}(p',q)$, which is the dominant one compare to, for example, the one-gluon exchange contribution.

Now we can substitute the propagator in Eq. (46) by the perturbative term of Eq. (40). Using the Particle Distribution Amplitudes (DAs) of ϕ in Appendix A.1 and contract the color index by the SU(N) algebra

$$
\varepsilon_{abc}\varepsilon_{dec}\delta_{ad}\delta_{bi}\delta_{ei} = -C_A(1-C_A) = 6, \tag{48}
$$

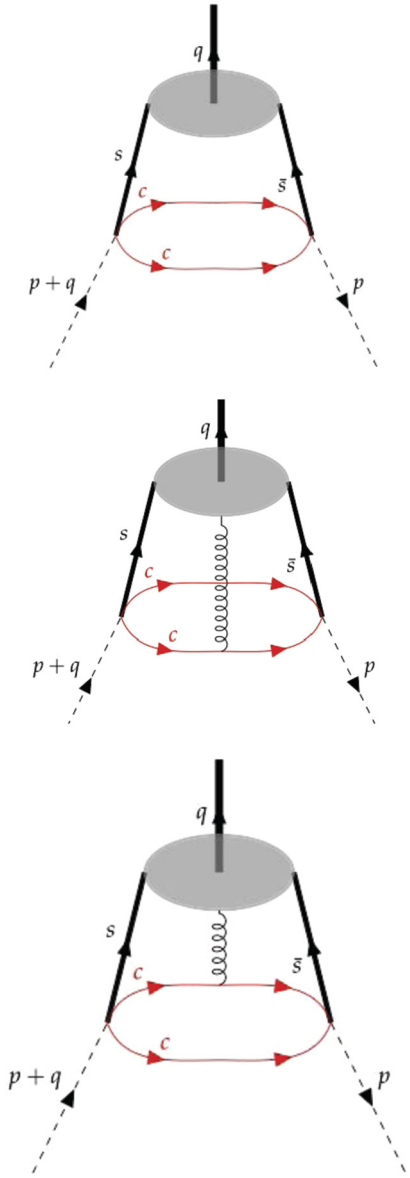

Fig. 1. The leading order and one-gluon exchange diagrams contribute to $\Pi_{(1),\mu}(p', q)$, which are the main contribution.

we will encounter four-dimensional integrals in the momentum spaces. After above operation, some terms in Eq. (46) will proportional to, for example

$$\int \frac{d^4k_1}{(2\pi)^4} \int \frac{d^4k_2}{(2\pi)^4} \frac{e^{-i(k_1-k_2)x} k_1 \cdot k_2}{(k_1^2 - m_c^2)(k_2^2 - m_c^2)} [(p \cdot q)\epsilon'_\mu - p \cdot \epsilon' q_\mu]. \tag{49}$$

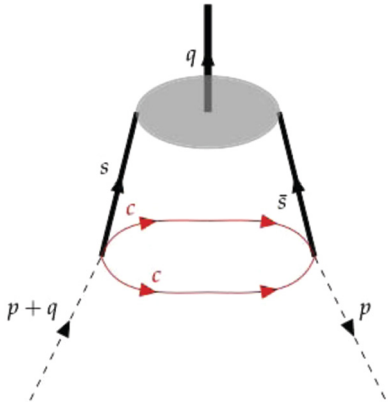

Fig. 2. The leading order diagram contribute to $\Pi_{\mu(2)}(p', q)$. The one-gluon exchange vanish in $\Pi_{(2),\mu}(p', q)$.

The main steps to calculate some four-dimensional integrals like (49) can be done by dimension regulation. Choose the structure proportional to ϵ'_μ, we can derive the corresponding spectral density

$$\begin{aligned}\rho^{\mathrm{OPE}}_{(1)}(\hat{s}) = &-\frac{f_\phi^{\parallel} m_\phi \sqrt{\hat{s}\left(\hat{s}-4m^2\right)}\left(2m^2+\hat{s}\right)}{12\pi^2\hat{s}} \\ &-\frac{f_\phi^{\parallel} m_c^2 m_\phi \langle \frac{\alpha_s}{\pi} GG\rangle \left(6m^2-\hat{s}\right)\sqrt{\hat{s}\left(\hat{s}-4m^2\right)}}{144\pi^2\hat{s}^2\left(\hat{s}-4m^2\right)^2} \\ &\frac{-\zeta_{4\phi}^{\perp} f_\phi^{\perp} m_c m_\phi^2 (2m_c^2-\hat{s})\sqrt{\hat{s}(\hat{s}-4m_c^2)}}{2\pi^2\hat{s}^2(4m_c^2-\hat{s})} + \frac{\tilde{\zeta}_{4\phi}^{\perp} f_\phi^{\perp} m_c m_\phi^2 \sqrt{\hat{s}(\hat{s}-4m_c^2)}}{2\pi^2\hat{s}(4m_c^2-\hat{s})},\end{aligned} \tag{50}$$

and

$$\rho^{\mathrm{OPE}}_{(2)}(\hat{s}) = \int_0^1 du u^2 \phi_2^{\perp}(u) \frac{\sqrt{2} m_c m_\phi^2 f_\phi^{\perp} \sqrt{\hat{s}(\hat{s}-4m_c^2)}}{2\pi^2\hat{s}}, \tag{51}$$

where m_ϕ and $f_\phi^{\perp}$ are the mass and decay constant of ϕ respectively. $\phi_2^{\perp}(u)$ is LCDA. $\zeta_4^{\perp}$ and $\tilde{\zeta}_4^{\perp}$ are three-particle distribution parameters defined in Appendix A.1, m_c is charm-quark mass. The strong coupling is then evaluated by Eq. (34). In addition, we can easily obtain the decay width of $X(4700) \to J/\psi\phi$ by applying the usual feynman diagram method [29]

$$\Gamma_{\mathrm{I}}(X(4700) \to J/\psi\phi) = \frac{(g_{XJ/\psi\phi})^2}{24\pi m_{\mathrm{I},X}^2} \lambda(m_{\mathrm{I},X}, m_{J/\psi}, m_\phi)\left(3 + \frac{\lambda(m_{\mathrm{I},X}, m_{J/\psi}, m_\phi)}{m_{J/\psi}^2}\right), \tag{52}$$

where

$$\lambda(a,b,c) = \frac{\sqrt{a^4+b^4+c^4-2*(a^2b^2+b^2c^2+c^2a^2)}}{2a}. \tag{53}$$

3. Numerical calculation

3.1. Input parameters

In this section, we analyze the numerical results for the coupling constant and the decay width of $X(4700) \to J/\psi\phi$, and present the mass and decay constant of $X(4700)$ as well. We adopt the following parameters for the numerical calculation. The current charm-quark mass, $m_c = (1.275 \pm 0.025)$ GeV, the J/ψ-meson mass $m_{J/\psi} = (3096.900 \pm 0.006)$ MeV and $\phi(980)$ mass $m_\phi = (990 \pm 20)$ MeV from the Particla Data Group (PDG) [24]. The J/ψ and $\phi(980)$ decay constants are taken as $f_{J/\psi} = 0.405$ GeV [29], $f_\phi = 0.18 \pm 0.015$ GeV [34]. The current-quark-mass for the s-quark is $m_s = 93^{+11}_{-5}$ MeV from PDG. The decay constants of ϕ is taken as $f_\phi^\parallel = 0.215$ GeV. The Gegenbauer moments, $a_1^\parallel = a_1^\perp = 0$ and $a_2^\parallel = 0.18$, $a_2^\perp = 0.14$ [35]. The parameters $\zeta_4^\perp$ and $\widetilde{\zeta}_4^\perp$ are taken as $\zeta_4^\perp = -0.01$ and $\widetilde{\zeta}_4^\perp = -0.03$ [35]. In addition, we also need to know the values of the non-perturbative vacuum condensates. The related parameters are [36]

$$\begin{aligned}
&\langle\bar{q}q\rangle = -(0.24 \pm 0.01)^3 \text{ GeV}^3, \\
&\langle\bar{s}s\rangle = (0.8 \pm 0.1) \times \langle\bar{q}q\rangle, \\
&\langle\frac{\alpha_s}{\pi}GG\rangle = (0.012) \text{ GeV}^4, \\
&\langle g_s\bar{s}\sigma Gs\rangle = m_0^2 \times \langle\bar{s}s\rangle, \\
&m_0^2 = 0.8 \text{ GeV}^2, \\
&m_c = 1.275 \pm 0.025 \text{ MeV}.
\end{aligned} \tag{54}$$

The sum rule predictions for the mass, the decay constant and the coupling constant depend on two parameters: Borel mass M^2 and continuum threshold s_0. The value of s_0 is being correlated with the onset of excited states of $X(4700)$. But according to the experimental data, there is no resonance activity related to the first excited states of $X(4700)$. We should turn to another way. From Table 1 which entail the masses calculations of charmonia and bottomonia, we can find the mass discrepancy between the ground state and first excited state are all around 0.5 GeV. Besides, the experimental data in Table 2 which extract from PDG prove most of the calculations in Table 1. Furthermore, one can refer to previous QCD sum rules caculations that assign $X(4140)$ and $X(4685)$ as the 1S and 2S tetraquark states respectively and that assign $Z_c(3900)$ and $Z_c(4430)$ as the 1S and 2S tetraquark states respectively and so on (see Table 3). The mass difference between the 1S and 2S tetraquark states are about $0.4 \sim 0.6$ GeV. So we accept the mass discrepancy and employ

$$(4.70 + 0.40)^2 \text{ GeV}^2 \leq s_0 \leq (4.70 + 0.60)^2 \text{ GeV}^2, \tag{55}$$

or rewrite it as

$$(5.20 - 0.10)^2 \text{ GeV}^2 \leq s_0 \leq (5.20 + 0.10)^2 \text{ GeV}^2. \tag{56}$$

After fixing s_0, we use two extra criteria to constrain the Borel mass M^2:

1. To obtain the minimal value of M^2, we require that the contribution of the condensates like $\langle\bar{q}g_sGq\rangle$ and higher dimension condensates in the OPE is smaller than 5% of the total contribution:

Table 1
Quark model masses calculated for the first three levels of charmonia and bottomonia [37].

Masses M(GeV) \ n	$c\bar{c}$			$b\bar{b}$		
	$n=1$	$n=2$	$n=3$	$n=1$	$n=2$	$n=3$
$M_{^3P_0}(\chi_{q0})$	3.37	3.88	4.30	9.81	10.2	10.7
$M_{^3P_1}(\chi_{q1})$	3.54	3.97	4.33	9.89	10.3	10.6
$M_{^1P_1}(h_q)$	3.53	3.96	4.37	9.88	10.3	10.6
$M_{^3P_2}(\chi_{q2})$	3.54	3.98	4.34	9.89	10.3	10.6

Table 2
Masses of experimentally observed states in Particle Data Group listings [38].

Masses $M(MeV)\backslash n$	$c\bar{c}$			$b\bar{b}$		
	$n=1$	$n=2$	$n=3$	$n=1$	$n=2$	$n=3$
$M_{^3P_0}(\chi_{q0})$	3414.75	–	–	9859.44	10232.5	–
$M_{^3P_1}(\chi_{q1})$	3510.66	–	–	9892.78	10255.46	10512.1
$M_{^1P_1}(h_q)$	3525.38	–	–	9899.3	10259.8	–
$M_{^3P_2}(\chi_{q2})$	3556.20	3922.5	–	9912.21	10268.65	–

Table 3
The mass difference between the 1S and 2S hidden-charm tetraquark states with the possible assignments [39].

J^{PC}	1S	2 S	Mass difference	References
1^{++}	$X(4140)$	$X(4685)$	566 MeV	[40,41]
1^{+-}	$Z_c(3900)$	$Z_c(4430)$	591 MeV	[42–44]
0^{++}	$X(3915)$	$X(4500)$	588 MeV	[45,19]
1^{+-}	$Z_c(4020)$	$Z_c(4600)$	576MeV	[46,47]

$$\mathrm{CVG} \equiv \left| \frac{\tilde{\Pi}_I^{\langle \bar{q} g_s G q \rangle + \cdots}\left(M^2, \infty\right)}{\tilde{\Pi}_I^{OPE}\left(M^2, \infty\right)} \right| \leq 5\%, \tag{57}$$

where dots denote higher dimension contributions.

2. Ensure that the one-pole in Eq. (5) is valid, we require that the pole contribution (PC) should be larger than 30% to determine the upper limit on M^2

$$\mathrm{PC} = \frac{\tilde{\Pi}_I^{OPE}(M^2, s_0)}{\tilde{\Pi}_I^{OPE}(M^2, \infty)} \geq 30\%. \tag{58}$$

As depicted in Fig. 3 and Fig. 4, CVG and PC decrease as M^2 grows higher. The green dot betokens that CVG turns into 30%, where the maximal Borel mass M^2 can be obtained. And the red dot present PC converges with 5% horizontal for $J^X_{(1)}$ and $J^X_{(2)}$, from which point, we can select the minimum Borel mass. Subsequently, we require the working region of the Borel parameter for mass and decay constant of $J^X_{(1)}$ to be in the region of

$$3.60\ \mathrm{GeV}^2 \leq M^2 \leq 4.13\ \mathrm{GeV}^2, \tag{59}$$

and $J^X_{(2)}$ to be in that of

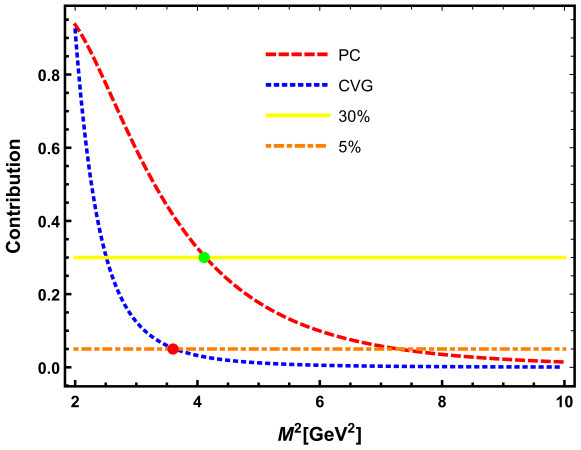

Fig. 3. Convergence (CVG) and pole contribution (PC) for $J^X_{(1)}$.

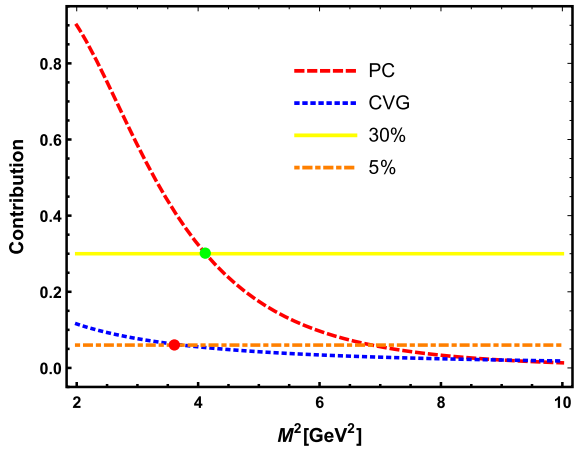

Fig. 4. Convergence (CVG) and pole contribution (PC) for $J^X_{(2)}$.

$$3.63\ \text{GeV}^2 \leq M^2 \leq 4.17\ \text{GeV}^2. \tag{60}$$

3.2. The mass and the decay constant

In Fig. 5 and Fig. 6 we present the results of the mass m^I_X and the decay constant f^I_X as functions of the parameters M^2 at fixed values of $s_0 \in \{(5.20-0.10)^2, (5.20+0.0)^2, (5.20+0.1)^2\}$. As we seen in the first figure in Fig. 5 and Fig. 6, the yellow curves correspond to the measurements of the Belle Collaboration [48] as shown in PDG. The blue, red and black curves show clear dependence of our prediction on s_0 and M^2. By choosing appropriate parameters, our predictions are consistent with the measurements. At a fixed point of $M^2 = 3.9\ \text{GeV}^2$, the masses of $J^X_{(1)}$ and $J^X_{(2)}$ are

$$m^{(1)}_X = 4.70^{+0.06}_{-0.05}\ \text{GeV}, \tag{61}$$

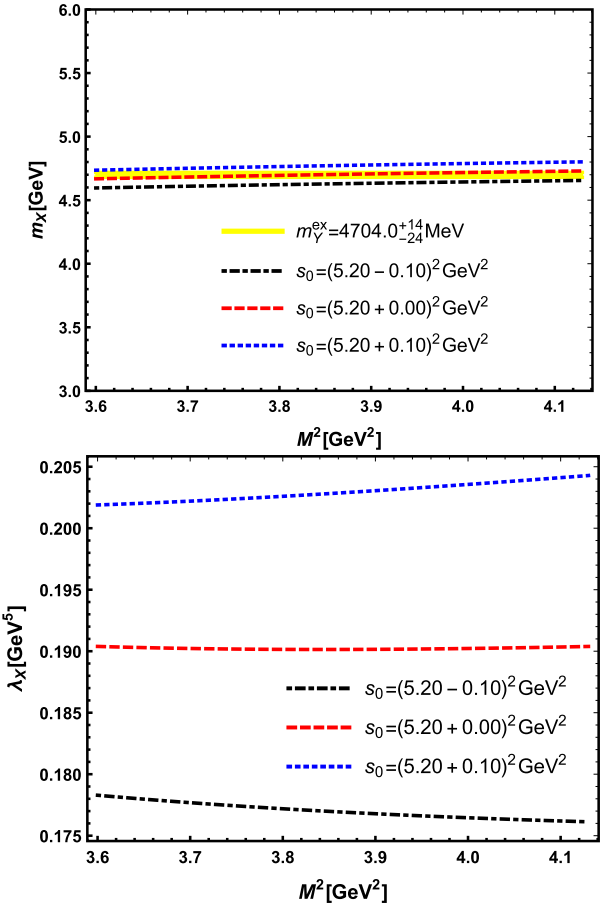

Fig. 5. The mass [first] and the decay constant [second] of a scalar tetraquark state $X(4700)$ as a function of the Borel parameter M^2 at different fixed values of s_0.

and

$$m_X^{(1)} = 4.67^{+0.04}_{-0.07}\ \text{GeV}, \tag{62}$$

respectively.

The uncertainty comes from the various condensates, and the strange and charm quark masses. Base on the Belle Collaboration measurements [48], $X(4700)$ has mass of $4704 \pm 10^{+14}_{-24}$ MeV. The predicted results of the two assignments are consistent with the experimental results. Therefore we can conclude that it might be a D-wave $cs\bar{c}\bar{s}$ tetraquark or a scalar tetraquark state. We then extend the same technique to evaluate the decay constant of $X(4700)$, the results of $J^X_{(1)}$ and $J^X_{(2)}$ at the same bench mark point reads

$$\lambda_X^{(1)} \equiv m_X^{(1)} f_X^{(1)} = 0.19^{+0.013}_{-0.014}\ \text{GeV}^5, \tag{63}$$

and

$$\lambda_X^{(2)} \equiv m_X^{(2)} f_X^{(2)} = 0.164^{+0.010}_{-0.011}\ \text{GeV}^7. \tag{64}$$

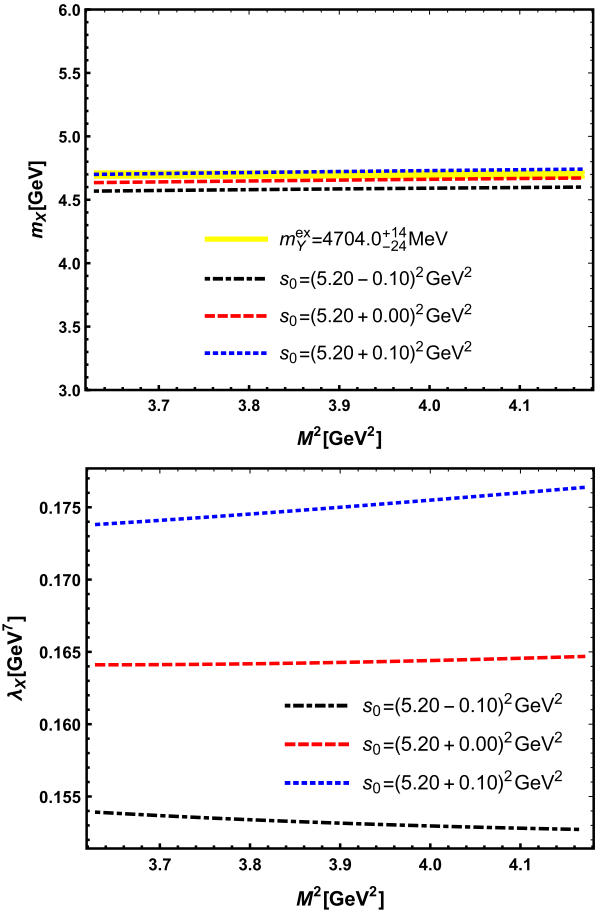

Fig. 6. The mass [first] and the decay constant [second] of a D-wave tetraquark state $X(4700)$ as a function of the Borel parameter M^2 at different fixed values of s_0.

The mass and decay constant given above will be used as input parameters to find the decay width of $X(4700) \to J/\psi\phi$.

3.3. The coupling constant and the decay width

We start to evaluate $g_{XJ/\psi\phi}$ and give the decay width of $X(4700) \to J/\psi\phi$ in order to confirm which hypotheses are more suitable. For M^2 and s_0, we use the same values as in the analysis of the mass. The result is shown in Fig. 7 and Fig. 8. Fig. 7 provides the result for the scalar tetraquark state. The parameters M^2 and s_0 are varied inside of the regions: $(3.60-4.13)^2$ GeV^2 and $(5.10-5.30)^2$ GeV^2. Our prediction for $g_{XJ/\psi\phi}$, take the average value, is

$$g_{XJ/\psi\phi} = 6.7^{+1.0}_{-0.8} \text{ GeV}. \tag{65}$$

The width of this decay can be obtained by Eq. (34):

$$\Gamma(X(4700) \to J/\psi\phi) = (109^{+35}_{-24}) \text{ MeV}. \tag{66}$$

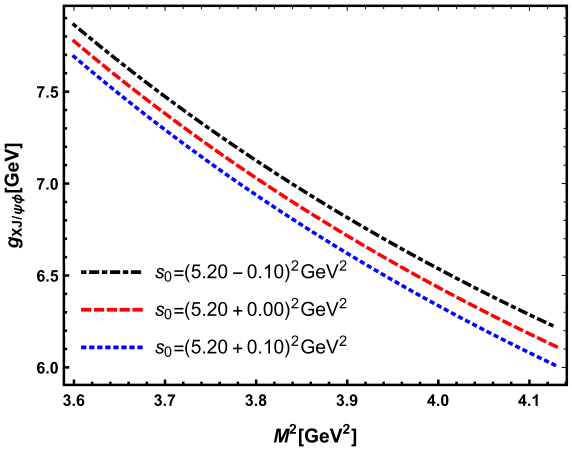

Fig. 7. The strong coupling $g_{XJ/\psi\phi}$ of a scalar tetraquark state $X(4700)$ as a function of the Borel parameter M^2 at different fixed values of s_0.

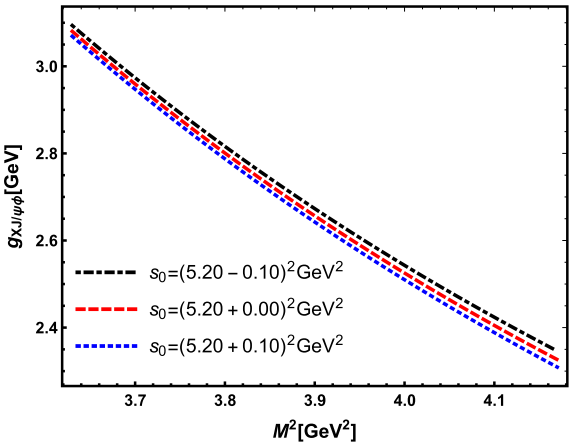

Fig. 8. The strong coupling $g_{XJ/\psi\phi}$ of a D-wave tetraquark state $X(4700)$ as a function of the Borel parameter M^2 at different fixed values of s_0.

The total width of $X(4700)$ from PDG [24] shows that

$$\Gamma(4700) = 120 \pm 31^{+42}_{-33}\ \text{MeV}, \tag{67}$$

which is close to our prediction within the error. The result seems like to indicate that if we assign $X(4700)$ as a scalar $cs\bar{c}\bar{s}$ tetraquark state then $X(4700) \to J/\psi\phi$ will the predominant process. However, since we only consider the hidden-charm meson decay channel in this paper, although the scalar tetraquark assignment yields a larger width when we compare it with the total width of $X(4700)$, this conclusion still has it's limitations before we consider the open-charm channels. The plan to calculate the open-charmed decay has been progressing, and those calculations will show us more information.

For D-wave tetraquark state, the results are shown in Fig. 8. The prediction for $g_{XJ/\psi\phi}$ is

$$g_{XJ/\psi\phi} = 2.65^{+0.44}_{-0.33}\ \text{GeV}. \tag{68}$$

The width of its decay can be obtained by Eq. (34) to be

$$\Gamma(X(4700) \to J/\psi\phi) = (17.1^{+6.2}_{-4.0})\ \text{MeV}, \tag{69}$$

which is much smaller than the width of $X(4700)$ in PDG.

4. Summary

In this work we assign $X(4700)$ as a D-wave tetraquark state and a scalar tetraquark state to study the mass and the decay constant of $X(4700)$, and also it's decay $X(4700) \to J/\psi\phi$. The mass of $X(4700)$ is evaluated through two-point sum rules, and both results of the two assignments are in agreement with the mass of $X(4700)$ in PDG. We also calculate the decay constant of $X(4700)$ in the SVZ sum rules. We then perform the calculation of the coupling constant $g_{XJ/\psi\phi}$ and the decay width by using the approach of the light-cone sum rules. We find that the scalar tetraquark assignment yields a larger width when we compare it with the total width of $X(4700)$, while being a D-wave tetraquark state, the decay of $X(4700) \to J/\psi\phi$ is much smaller. Since we only consider the hidden-charm meson decay channel in this paper, although the scalar tetraquark assignment yields a larger width when we compare it with the total width of $X(4700)$, we can not conclude that $X(4700) \to J/\psi\phi$ should the predominant process before we consider the open-charm channels.

CRediT authorship contribution statement

Yiling Xie: Data curation, Writing – original draft. **Dazhuang He:** Investigation. **Xuan Luo:** Investigation, Visualization. **Hao Sun:** Conceptualization, Methodology, Supervision, Writing – review & editing.

Declaration of competing interest

The authors declare that they have no known competing financial interests or personal relationships that could have appeared to influence the work reported in this paper.

Data availability

Data will be made available on request.

Appendix A

A.1. The relations between the light-cone distribution amplitudes (LCDAs) and the matrix elements

The matrix elements of the ϕ can be expanded in terms of the corresponding distribution amplitudes. Here we provide the expressions for the $\langle\phi(P)|\bar{q}(0)\Gamma^a q(0)|0\rangle$ type matrix elements [49]:

$$\left\langle \phi(P,\lambda) \left| \bar{q}(0)\gamma_\mu q(0) \right| 0 \right\rangle = f_\phi^{\parallel} m_\phi \epsilon_\mu^{*(\lambda)} \tag{70}$$

$$\left\langle \phi(P,\lambda) \left| \bar{q}(0)\sigma_{\mu\nu} q(0) \right| 0 \right\rangle = i f_\phi^{\perp} \left(e_\mu^{*(\lambda)} P_\nu - e_\nu^{*(\lambda)} P_\mu \right). \tag{71}$$

We also provide the expressions for $\langle\phi(P)|\bar{q}(0)gG_{\alpha\beta}\Gamma^a q(0)|0\rangle$ type matrix elements [35,50]:

$$\begin{aligned}\left\langle\phi(P,\lambda)\left|\bar{q}(0)g\widetilde{G}_{\alpha\beta}\gamma_\mu\gamma_5 q(0)\right|0\right\rangle &= f_\phi^{\parallel}m_\phi\zeta_{3\phi}^{\parallel}[e_\alpha^{(\lambda)}\left(P_\beta P_\mu-\frac{1}{3}m_\phi^2 g_{\beta\mu}\right)-(\alpha\leftrightarrow\beta)] \\ &+\frac{1}{3}f_\phi^{\parallel}m_\phi^3\zeta_{4\phi}^{\parallel}\left(e_\alpha^{(\lambda)}g_{\beta\mu}-e_\beta^{(\lambda)}g_{\alpha\mu}\right), \end{aligned} \tag{72}$$

$$\begin{aligned}\left\langle\phi(P,\lambda)\left|\bar{q}(0)gG_{\alpha\beta}i\gamma_\mu q(0)\right|0\right\rangle &= -f_\phi^{\parallel}m_\phi\kappa_{3\phi}^{\parallel}[e_\alpha^{(\lambda)}\left(P_\beta P_\mu-\frac{1}{3}m_\phi^2 g_{\beta\mu}\right)-(\alpha\leftrightarrow\beta)] \\ &-\frac{1}{3}f_\phi^{\parallel}m_\phi^3\kappa_{4\phi}^{\parallel}\left(e_\alpha^{(\lambda)}g_{\beta\mu}-e_\beta^{(\lambda)}g_{\alpha\mu}\right), \end{aligned} \tag{73}$$

$$\left\langle\phi(P,\lambda)\left|\bar{q}(0)gG_{\alpha\beta}q(0)\right|\right\rangle = -if_\phi^{\perp}m_\phi^2\zeta_{4\phi}^{\perp}\left(\epsilon_\alpha^{(\lambda)}P_\beta-\epsilon_\beta^{(\lambda)}P_\alpha\right), \tag{74}$$

$$\left\langle\phi(P,\lambda)\left|\bar{q}(0)g\widetilde{G}_{\alpha\beta}\gamma_5 q(0)\right|0\right\rangle = f_\phi^{\perp}m_\phi^2\widetilde{\zeta}_{4\phi}^{\perp}\left(\epsilon_\alpha^{(\lambda)}P_\beta-\epsilon_\beta^{(\lambda)}P_\alpha\right), \tag{75}$$

$$\begin{aligned}\left\langle\phi(P,\lambda)\left|\bar{q}(0)gG_{\alpha\mu}\sigma_{\beta\mu}q(0)\right|\right\rangle &= f_\phi^{\perp}m_\phi^2[\frac{1}{2}\kappa_{3\phi}^{\perp}\left(\epsilon_\alpha^{(\lambda)}P_\beta+\epsilon_\beta^{(\lambda)}P_\alpha\right) \\ &+\kappa_{4\phi}^{\perp}\left(\epsilon_\alpha^{(\lambda)}P_\beta-\epsilon_\beta^{(\lambda)}P_\alpha\right)], \end{aligned} \tag{76}$$

where the dual gluon field strength tensor is defined as $\widetilde{G}_{\mu\nu}=\frac{1}{2}\epsilon_{\mu\nu\rho\sigma}G^{\rho\sigma}$. The generic notations of ζ are G-conserving and κ are G-breaking parameters. $\zeta_{3\phi}$, $\widetilde{\zeta}_{3\phi}$, $\kappa_{3\phi}$ are twist-3 and $\zeta_{4\phi}$, $\widetilde{\zeta}_{4\phi}$, $\kappa_{4\phi}$ are twist-4 parameters given in [35].

The covariant derivative is defined as

$$\overleftarrow{D}_\mu=\partial_\mu+igT^aA_\mu^a, \tag{77}$$

and it is also valid in the Fock-Schwinger gauge

$$x^\mu A_\mu^a(x)=0, \tag{78}$$

after performing some deduction, we can derive the following relations [51]:

$$A_\mu^a(x)=\frac{1}{2}x^v G_{v\mu}^a(0)+\frac{1}{3}x^v x^\alpha\left[D_\alpha G_{v\mu}(0)\right]^a+\frac{1}{8}x^v x^\alpha x^\beta\left[D_\alpha D_\beta G_{v\mu}(0)\right]^a+\cdots. \tag{79}$$

Therefore, insert the gluonic fields back to the covariant derivative and calculate $\langle\phi(P)|\bar{q}(0)\overleftarrow{D}_\mu\overleftarrow{D}_v\Gamma^a q(0)|0\rangle$, we obtain the desired results:

$$\begin{aligned}\langle\phi(P)|\bar{q}(0)\overleftarrow{D}_\mu\overleftarrow{D}_v\Gamma^a q(0)|0\rangle &= \langle\phi(P)|\partial_\mu\partial_v[\bar{q}(x)]|_{x=0}\Gamma^a q(0)|0\rangle \\ &+\langle\phi(P)|\bar{q}(0)\frac{igT^b}{2}G_{\mu v}^b\Gamma^a q(0)|0\rangle \\ &=\partial_\mu\partial_v[\langle\phi(P)|\bar{q}(x)\Gamma^a q(0)|0\rangle]|_{x=0} \\ &+\frac{i}{2}\langle\phi(P)|\bar{q}(0)gG_{\mu v}\Gamma^a q(0)|0\rangle, \end{aligned} \tag{80}$$

where $\langle\phi(P)|\bar{q}(0)gG_{\mu v}\Gamma^a q(0)|0\rangle$ type matrix elements are given before. In addition, $\langle\phi(P)|\bar{q}(x)\Gamma^a q(0)|0\rangle$ type expressions are provided below [49]:

$$\left\langle \phi(P,\lambda)\left|\bar{q}(x)\sigma_{\rho\nu}q(0)\right|0\right\rangle = -i\left(e_\rho^{(\lambda)}P_\nu - e_\nu^{(\lambda)}P_\rho\right)\times f_\phi^\perp\int_0^1 du e^{iupx}\phi_2^\perp(u,\mu), \tag{81}$$

$$\langle \phi(P,\lambda)\left|\bar{q}(x)\gamma_\theta\gamma_5 q(0)\right|0\rangle = -\frac{1}{4}\epsilon_{\theta\nu\rho\sigma}e^{(\lambda)\nu}P^\rho x^\sigma f_\phi m_\phi\times\int_0^1 du e^{iupx}g_\perp^{(a)}(u,\mu), \tag{82}$$

$$\begin{aligned}\left\langle \phi(P,\lambda)\left|\bar{q}(x)\gamma_\rho q(0)\right|0\right\rangle &= P_\rho\left(e^{(\lambda)}x\right)f_\phi m_\phi\times\int_0^1 du e^{iupx}\Phi_\parallel(u,\mu)\\ &+ e_\rho^{(\lambda)}f_\phi m_\phi\int_0^1 du e^{iupx}g_\perp^{(v)}(u,\mu),\end{aligned} \tag{83}$$

where

$$g_\perp^{(v),\text{ twist }2}(u,\mu) = \frac{1}{2}\left[\int_0^u dy\frac{\phi_2^\parallel(y,\mu)}{\bar{y}} + \int_u^1 dy\frac{\phi_2^\parallel(y,\mu)}{y}\right], \tag{84}$$

$$g_\perp^{(a),\text{ twist }2}(u,\mu) = 2\left[\bar{u}\int_0^u dy\frac{\phi_2^\parallel(y,\mu)}{\bar{y}} + u\int_u^1 dy\frac{\phi_2^\parallel(y,\mu)}{y}\right], \tag{85}$$

and

$$\Phi_\parallel(u,\mu) = \frac{1}{2}\left[\bar{u}\int_0^u dy\frac{\phi_2^\parallel(y,\mu)}{\bar{y}} - u\int_u^1 dy\frac{\phi_2^\parallel(y,\mu)}{y}\right]. \tag{86}$$

Here $\bar{u}=1-u$, $\bar{y}=1-y$. In term of Gegenbauer polynomials, $\phi_2^{\parallel,\perp}$ is given as [35]

$$\phi_2^{\parallel,\perp}(u,\mu) = 6u\bar{u}\left\{1+\sum_{n=1}^\infty a_n^{\parallel,\perp}(\mu)C_n^{3/2}(2u-1)\right\}, \tag{87}$$

the Gegenbauer polynomials $C_n^{3/2}(x)$ and coefficients a_n at the renormalization scale μ are given in details in [49].

A.2. Spectral densities

In this section we provide the spectral densities for $J_{(1)}$ and $J_{(2)}$. In the following expressions, $\mathrm{H}(x)$ is defined as:

$$\mathrm{H}(x) = \begin{cases}0 & x\geq 0\\ 1 & x<0.\end{cases} \tag{88}$$

The spectral density for $J_{(1)}$ can be divide into:

$$\begin{aligned}\tilde{\rho}_{(1)}^{OPE}(\hat{s}) &= \tilde{\rho}_{(1)}^{pert}(\hat{s}) + \tilde{\rho}_{(1)}^{\langle\bar{q}q\rangle}(\hat{s}) + \tilde{\rho}_{(1)}^{\langle\frac{\alpha_s}{\pi}GG\rangle}(\hat{s})\\ &+ \tilde{\rho}_{(1)}^{\langle\bar{q}g_s\sigma Gq\rangle}(\hat{s}) + \tilde{\rho}_{(1)}^{\langle\bar{q}q\rangle^2}(\hat{s}) + \tilde{\rho}_{(1)}^{\langle\frac{\alpha_s}{\pi}GG\rangle\langle\bar{q}q\rangle}(\hat{s})\end{aligned} \tag{89}$$

with

$$\begin{aligned}\tilde{\rho}_{(1)}^{pert}(\hat{s}) = &\int_0^1 dx \int_0^1 dy \frac{y\left(m_c^2+\hat{s}x(x(-y)+x+y-1)\right)^2}{768\pi^6(x-1)^3x^3(y-1)^3}\\
&\times\Big(m^4y\left(3y^3+7y^2-3y+3\right)-12m_c^3m_sy\left(y^2-1\right)\\
&-2m_c^2(x-1)x(y-1)(36m_s^2(y-1)\\
&+\hat{s}y(9y^3+20y^2+9y+6))\\
&+30m_cm_s\hat{s}(x-1)x(y-1)^2y(y+1)\\
&+3\hat{s}^2(x-1)^2x^2(y-1)^2y(7y^3+15y^2+9y+3)\Big)\\
&\times \mathrm{H}\left(y\left(x\hat{s}(x(-y)+x+y-1)+m_c^2\right)\right), \qquad (90)\\
\tilde{\rho}_{(1)}^{\langle\bar{q}q\rangle}(\hat{s}) = &-\int_0^1 dx \int_0^1 dy \frac{\langle\bar{q}q\rangle}{16\pi^4(x-1)^2x^2(y-1)}\\
&\times\Big(2m^5y(y+1)-2m^4\mathrm{mq}(x-1)x\left(3y^3+5y^2-3y+5\right)\\
&+2m_c^3(x-1)x\left(y^2-1\right)\left(m_s^2-3\hat{s}y\right)\\
&+2m_c^2m_s\hat{s}(x-1)^2x^2\left(12y^4+9y^3-15y^2+y-7\right)\\
&+m\hat{s}(x-1)^2x^2(y-1)^2(y+1)\left(4\hat{s}y-3m_q^2\right)\\
&-4m_s\hat{s}^2(x-1)^3x^3(y-1)^2\left(5y^3+9y^2+5y+1\right)\Big)\\
&\times \mathrm{H}\left(y\left(x\hat{s}(x(-y)+x+y-1)+m_c^2\right)\right), \qquad (91)\\
\tilde{\rho}_{(1)}^{\langle\frac{\alpha_s}{\pi}GG\rangle}(\hat{s}) = &\int_0^1 dx \int_0^1 dy \frac{\langle\frac{\alpha_s}{\pi}GG\rangle}{512\pi^4(x-1)x(y-1)}\\
&\Big(\times m_c^4\left(3y^3+7y^2+y+1\right)\\
&-m^2\hat{s}(x-1)x\left(12y^4+15y^3-17y^2-7y-3\right)\\
&+2\hat{s}^2(x-1)^2x^2(y-1)^2\left(5y^3+11y^2+5y+1\right)\Big)\\
&\times\mathrm{H}\left(y\left(x\hat{s}(x(-y)+x+y-1)+m_c^2\right)\right),\\
\tilde{\rho}_{(1)}^{\langle\bar{q}g_s\sigma Gq\rangle}(\hat{s}) = &\int_0^1 dx \int_0^1 dy \frac{\langle\bar{q}g_s\sigma Gq\rangle}{192\pi^4(x-1)x}\\
&\times\Big(2m_c^3(2x-7)(y+1)\\
&+8m_c^2m_s(x-1)x\left(3y^2+4y+3\right)\end{aligned}$$

$$
\begin{aligned}
&-3m_c\hat{s}\left(2x^2-9x+7\right)x\left(y^2-1\right)\\
&-24m_s\hat{s}(x-1)^2x^2\left(2y^3+y^2-y-2\right)\Big)\\
&\times\mathrm{H}\left(y\left(x\hat{s}(x(-y)+x+y-1)+m_c^2\right)\right)\\
&+\int_0^1 dx\left(\frac{\langle\bar{q}g_s\sigma Gq\rangle\left(64m_c^2m_s-8m_s\hat{s}x(x+3)\right)}{384\pi^4}\right.\\
&\left.+\frac{\langle\bar{q}g_s\sigma Gq\rangle\left(m\left(-2m_0x+m_0+8m_s^2\right)\right)}{384\pi^4}\right)\\
&\times\mathrm{H}(m^2-x(x+1)s),
\end{aligned}
\tag{92}
$$

$$
\begin{aligned}
\tilde{\rho}_{(1)}^{\langle\bar{q}q\rangle^2}(\hat{s}) = &\int_0^1 dx\int_0^1 dy\mathrm{H}\left(y\left(x\hat{s}(x(-y)+x+y-1)+m_c^2\right)\right)\\
&\times(-\frac{g_s^2\langle\bar{q}q\rangle^2\left(m_c^2\left(3y^2+4y+3\right)\right)}{162\pi^4}\\
&-\frac{g_s^2\langle\bar{q}q\rangle^2\left(-3\hat{s}(x-1)x\left(2y^3+y^2-y-2\right)\right)}{162\pi^4})\\
&+\int_0^1 dx\frac{\langle\bar{q}q\rangle^2}{324\pi^4}\mathrm{H}(m^2-x(x+1)s)\\
&\times\left(g_s^2\left(-2m_c^2-m_cm_s+\hat{s}(x+3)x\right)\right.\\
&\left.+27\pi^2\left(4m_c^2+2m_cm_s-m_s^2(x-6)x\right)\right),
\end{aligned}
\tag{93}
$$

$$
\begin{aligned}
\tilde{\rho}_{(1)}^{\langle\frac{\alpha_s}{\pi}GG\rangle\langle\bar{q}q\rangle}(\hat{s}) = &\int_0^1 dx\frac{im_c\langle\frac{\alpha_s}{\pi}GG\rangle\langle\bar{q}q\rangle}{144\pi^3}\\
&\mathrm{H}\left(m^2-x(x+1)s\right).
\end{aligned}
\tag{94}
$$

The spectral density for $J_{(2)}$ can be divide into:

$$
\begin{aligned}
\tilde{\rho}_{(2)}^{OPE}(\hat{s}) = &\tilde{\rho}_{(2)}^{\langle\frac{\alpha_s}{\pi}GG\rangle}(\hat{s})+\tilde{\rho}_{(2)}^{\langle\bar{q}g_s\sigma Gq\rangle}(\hat{s})+\tilde{\rho}_{(2)}^{\langle\frac{\alpha_s}{\pi}GG\rangle\langle\bar{q}q\rangle}(\hat{s})+\tilde{\rho}_{(2)}^{\langle\bar{q}g_s\sigma Gq\rangle\langle\bar{q}q\rangle}(\hat{s})\\
&+\tilde{\rho}_2^{\langle\bar{q}g_s\sigma Gq\rangle\langle\frac{\alpha_s}{\pi}GG\rangle}(\hat{s})+\tilde{\rho}_{(2)}^{\langle\bar{q}q\rangle^2\langle\frac{\alpha_s}{\pi}GG\rangle}(\hat{s})
\end{aligned}
\tag{95}
$$

with

$$
\begin{aligned}
\tilde{\rho}_{(2)}^{\langle\frac{\alpha_s}{\pi}GG\rangle}(\hat{s}) = &\int_0^1\int_0^1 dxdy\frac{i\langle\frac{\alpha_s}{\pi}GG\rangle y^2}{9216\pi^4(x-1)^4x^3(y-1)^3}\\
&\times\left(m^8\left(2x\left(18y^4+54y^3+49y^2+33y-3\right)\right.\right.\\
&\left.\left.+36y^4+117y^3+109y^2+34y+6\right)\right.
\end{aligned}
$$

$$
\begin{aligned}
&-12m_c^6\hat{s}x(y-1)\left(x^2\left(30y^4+84y^3+79y^2+38y-3\right)\right.\\
&+2x\left(3y^3+2y^2-7y+2\right)\\
&\left.-30y^4-90y^3-83y^2-24y-1\right)\\
&+12m_c^4\hat{s}^2(x-1)^2x^2(y-1)^2\\
&\times\left(x\left(90y^4+240y^3+224y^2+90y-6\right)\right.\\
&\left.+\left(90y^3+255y^2+229y+64\right)y\right)\\
&-4m_c^2\hat{s}^3(x-1)^3x^3(y-1)^3\\
&\times\left(x\left(315y^4+810y^3+740y^2+264y-15\right)\right.\\
&\left.+315y^4+855y^3+745y^2+202y-3\right)\\
&+3\hat{s}^4(x-1)^4x^4(y-1)^4\\
&\times\left(2x\left(84y^4+210y^3+187y^2+61y-3\right)\right.\\
&\left.+\ +168y^4+441y^3+373y^2+98y-2\right)\Big)\\
&\times\mathrm{H}\left(y\left(x\hat{s}(x(-y)+x+y-1)+m_c^2\right)\right),
\end{aligned}
\tag{96}
$$

$$
\begin{aligned}
\tilde{\rho}_{(2)}^{\langle\bar{q}g_s\sigma Gq\rangle}(\hat{s}) = &\int_0^1\int_0^1 dxdy\frac{5m_s\langle\bar{q}g_s\sigma Gq\rangle}{576\pi^4(x-1)^2x^2(y-1)^2}\\
&\times2\left(m_c^6\left(6y^3+7y^2+8y-1\right)y\right.\\
&-m_c^4(x-1)x(y-1)\left(3sy\left(24y^3+33y^2+26y-3\right)\right.\\
&\left.-m_0\left(12y^3+15y^2+14y-1\right)\right)\\
&+m_c^2\hat{s}(x-1)^2x^2(y-1)^2\left(12\hat{s}y\left(10y^3+15y^2+10y-1\right)\right.\\
&\left.-m_0\left(48y^3+69y^2+50y-3\right)\right)\\
&+\hat{s}^2(x-1)^3x^3(y-1)^3\left(m_0\left(40y^3+62y^2+40y-2\right)\right.\\
&\left.\left.-\hat{s}y\left(60y^3+95y^2+58y-5\right)\right)\right)\\
&\times\mathrm{H}\left(y\left(x\hat{s}(x(-y)+x+y-1)+m_c^2\right)\right),
\end{aligned}
\tag{97}
$$

$$
\begin{aligned}
\tilde{\rho}_{(2)}^{\langle\frac{\alpha_s}{\pi}GG\rangle\langle\bar{q}q\rangle}(\hat{s}) = &\int_0^1\int_0^1 dxdy\mathrm{H}\left(y\left(x\hat{s}(x(-y)+x+y-1)+m_c^2\right)\right)\\
&\times\frac{-m_c\langle\frac{\alpha_s}{\pi}GG\rangle\langle\bar{q}q\rangle\left(m_c^2+\hat{s}x(x(-y)+x+y-1)\right)}{16\pi^2(x-1)^2x(y-1)}
\end{aligned}
$$

$$\times \Big(m_c^2(y+1)y + 2m_c m_s(x-1)(y-1) - 2\hat{s}(x-1)xy\left(y^2-1\right)\Big), \tag{98}$$

$$\tilde{\rho}_{(2)}^{\langle\bar{q}g_s\sigma Gq\rangle\langle\bar{q}q\rangle}(\hat{s}) = \int_0^1\int_0^1 dxdy\mathrm{H}\left(y\left(x\hat{s}(x(-y)+x+y-1)+m_c^2\right)\right) \times\frac{-5g_s^2\langle\bar{q}g_s\sigma Gq\rangle\langle\bar{q}q\rangle}{3888\pi^4(x-1)x(y-1)} \times\Big(m_c^4\left(12y^3+15y^2+14y-1\right) -m_c^2\hat{s}(x-1)x\left(48y^4+21y^3-19y^2-53y+3\right) +2\hat{s}^2(x-1)^2x^2(y-1)^2\left(20y^3+31y^2+20y-1\right)\Big), \tag{99}$$

$$\tilde{\rho}_{2}^{\langle\bar{q}g_s\sigma Gq\rangle\langle\frac{\alpha_s}{\pi}GG\rangle}(\hat{s}) = \int_0^1\int_0^1 dxdy\mathrm{H}\left(y\left(x\hat{s}(x(-y)+x+y-1)+m_c^2\right)\right) \times\Bigg(-\frac{5\langle\frac{\alpha_s}{\pi}GG\rangle m_c\langle\bar{q}g_s\sigma Gq\rangle(y+1)\left(2m^2\right)}{768\pi^2(x-1)} -\frac{5\langle\frac{\alpha_s}{\pi}GG\rangle m_c\langle\bar{q}g_s\sigma Gq\rangle}{768\pi^2(x-1)} \times(y+1)\left(3\hat{s}x(x(-y)+x+y-1)\right)\Bigg), \tag{100}$$

$$\tilde{\rho}_{(2)}^{\langle\bar{q}q\rangle^2\langle\frac{\alpha_s}{\pi}GG\rangle}(\hat{s}) = \int_0^1 dx\mathrm{H}\left(m_c^2-x(x+1)\hat{s}\right) \times\frac{1}{6}\langle\frac{\alpha_s}{\pi}GG\rangle m_c^2\langle\bar{q}q\rangle^2 - \frac{1}{12}\langle\frac{\alpha_s}{\pi}GG\rangle m_c m_s\langle\bar{q}q\rangle^2 x. \tag{101}$$

References

[1] R. Aaij, et al., Observation of $J/\psi\phi$ structures consistent with exotic states from amplitude analysis of $B^+ \to J/\psi\phi K^+$ decays, Phys. Rev. Lett. 118 (2) (2017) 022003, https://doi.org/10.1103/PhysRevLett.118.022003, arXiv:1606.07895.

[2] R. Aaij, et al., Amplitude analysis of $B^+ \to J/\psi\phi K^+$ decays, Phys. Rev. D 95 (1) (2017) 012002, https://doi.org/10.1103/PhysRevD.95.012002, arXiv:1606.07898.

[3] S.S. Agaev, K. Azizi, H. Sundu, Exploring the resonances X(4140) and X(4274) through their decay channels, Phys. Rev. D 95 (2017) 114003, https://doi.org/10.1103/PhysRevD.95.114003.

[4] L.-C. Gui, L.-S. Lu, Q.-F. Lü, X.-H. Zhong, Q. Zhao, Strong decays of higher charmonium states into open-charm meson pairs, Phys. Rev. D 98 (1) (2018) 016010, https://doi.org/10.1103/PhysRevD.98.016010, arXiv:1801.08791.

[5] F. Fernández, D.R. Entem, P.G. Ortega, J. Segovia, From J/ψ to LHCb pentaquarks, PoS CHARM2016 (2016) 054, https://doi.org/10.22323/1.289.0054, arXiv:1611.08534.

[6] P.G. Ortega, J. Segovia, D.R. Entem, F. Fernández, Canonical description of the new LHCb resonances, Phys. Rev. D 94 (11) (2016) 114018, https://doi.org/10.1103/PhysRevD.94.114018, arXiv:1608.01325.

[7] R. Oncala, J. Soto, Heavy quarkonium hybrids: spectrum, decay and mixing, Phys. Rev. D 96 (1) (2017) 014004, https://doi.org/10.1103/PhysRevD.96.014004, arXiv:1702.03900.

[8] S. Ozaki, S. Sasaki, Lüscher's finite size method with twisted boundary conditions: an application to the J/ψ-ϕ system to search for a narrow resonance, Phys. Rev. D 87 (1) (2013) 014506, https://doi.org/10.1103/PhysRevD.87.014506, arXiv:1211.5512.

[9] J.Y. Panteleeva, I.A. Perevalova, M.V. Polyakov, P. Schweitzer, Tetraquarks with hidden charm and strangeness as ϕ-$\psi(2S)$ hadrocharmonium, Phys. Rev. C 99 (4) (2019) 045206, https://doi.org/10.1103/PhysRevC.99.045206, arXiv:1802.09029.

[10] L. Maiani, A.D. Polosa, V. Riquer, Interpretation of axial resonances in J/psi-phi at LHCb, Phys. Rev. D 94 (5) (2016) 054026, https://doi.org/10.1103/PhysRevD.94.054026, arXiv:1607.02405.

[11] Q.-F. Lü, Y.-B. Dong, X(4140), X(4274), X(4500), and X(4700) in the relativized quark model, Phys. Rev. D 94 (7) (2016) 074007, https://doi.org/10.1103/PhysRevD.94.074007, arXiv:1607.05570.

[12] R. Zhu, Hidden charm octet tetraquarks from a diquark-antidiquark model, Phys. Rev. D 94 (5) (2016) 054009, https://doi.org/10.1103/PhysRevD.94.054009, arXiv:1607.02799.

[13] C. Deng, J. Ping, H. Huang, F. Wang, Hidden charmed states and multibody color flux-tube dynamics, Phys. Rev. D 98 (1) (2018) 014026, https://doi.org/10.1103/PhysRevD.98.014026, arXiv:1801.00164.

[14] J. Wu, Y.-R. Liu, K. Chen, X. Liu, S.-L. Zhu, $X(4140)$, $X(4270)$, $X(4500)$ and $X(4700)$ and their $cs\bar{c}\bar{s}$ tetraquark partners, Phys. Rev. D 94 (9) (2016) 094031, https://doi.org/10.1103/PhysRevD.94.094031, arXiv:1608.07900.

[15] Y. Yang, J. Ping, Investigation of $cs\bar{c}\bar{s}$ tetraquark in the chiral quark model, Phys. Rev. D 99 (9) (2019) 094032, https://doi.org/10.1103/PhysRevD.99.094032, arXiv:1903.08505.

[16] M.N. Anwar, J. Ferretti, E. Santopinto, Spectroscopy of the hidden-charm $[qc][\bar{q}\bar{c}]$ and $[sc][\bar{s}\bar{c}]$ tetraquarks in the relativized diquark model, Phys. Rev. D 98 (9) (2018) 094015, https://doi.org/10.1103/PhysRevD.98.094015, arXiv:1805.06276.

[17] X. Liu, H. Huang, J. Ping, D. Chen, X. Zhu, The explanation of some exotic states in the $cs\bar{c}\bar{s}$ tetraquark system, Eur. Phys. J. C 81 (10) (2021) 950, https://doi.org/10.1140/epjc/s10052-021-09752-y, arXiv:2103.12425.

[18] H.-X. Chen, E.-L. Cui, W. Chen, X. Liu, S.-L. Zhu, Understanding the internal structures of the $X(4140)$, $X(4274)$, $X(4500)$ and $X(4700)$, Eur. Phys. J. C 77 (3) (2017) 160, https://doi.org/10.1140/epjc/s10052-017-4737-5, arXiv:1606.03179.

[19] Z.-G. Wang, Scalar tetraquark state candidates: $X(3915)$, $X(4500)$ and $X(4700)$, Eur. Phys. J. C 77 (2) (2017) 78, https://doi.org/10.1140/epjc/s10052-017-4640-0, arXiv:1606.05872.

[20] L.J. Reinders, H. Rubinstein, S. Yazaki, Hadron properties from QCD sum rules, Phys. Rep. 127 (1985) 1, https://doi.org/10.1016/0370-1573(85)90065-1.

[21] S.X. Nakamura, X structures in $B^+ \to J/\psi\phi K^+$ as one-loop and double-triangle threshold cusps, arXiv:2111.05115, 2021.

[22] X.-H. Liu, How to understand the underlying structures of $X(4140)$, $X(4274)$, $X(4500)$ and $X(4700)$, Phys. Lett. B 766 (2017) 117–124, https://doi.org/10.1016/j.physletb.2017.01.008, arXiv:1607.01385.

[23] Y.-H. Ge, X.-H. Liu, H.-W. Ke, Threshold effects as the origin of $Z_{cs}(4000)$, $Z_{cs}(4220)$ and $X(4700)$ observed in $B^+ \to J/\psi\phi K^+$, arXiv:2103.05282, 2021, https://doi.org/10.1140/epjc/s10052-021-09590-y.

[24] P.A. Zyla, et al., Review of particle physics, Prog. Theor. Exp. Phys. 2020 (8) (2020) 083C01, https://doi.org/10.1093/ptep/ptaa104.

[25] R.M. Albuquerque, M. Nielsen, QCD sum rules study of the J(PC) = 1– charmonium Y mesons, Nucl. Phys. A 815 (2009) 53–66, https://doi.org/10.1016/j.nuclphysa.2011.04.001, Erratum: Nucl. Phys. A 857 (2011) 48–49, arXiv:0804.4817.

[26] D. Bečirević, G. Duplančić, B. Klajn, B. Melić, F. Sanfilippo, Lattice QCD and QCD sum rule determination of the decay constants of η_c, J/ψ and h_c states, Nucl. Phys. B 883 (2014) 306–327, https://doi.org/10.1016/j.nuclphysb.2014.03.024, arXiv:1312.2858.

[27] V.M. Belyaev, V.M. Braun, A. Khodjamirian, R. Ruckl, $D^*D\pi$ and $B^*B\pi$ couplings in QCD, Phys. Rev. D 51 (1995) 6177–6195, https://doi.org/10.1103/PhysRevD.51.6177, arXiv:hep-ph/9410280.

[28] B.L. Ioffe, A.V. Smilga, Nucleon magnetic moments and magnetic properties of vacuum in QCD, Nucl. Phys. B 232 (1984) 109–142, https://doi.org/10.1016/0550-3213(84)90364-X.

[29] J.M. Dias, F.S. Navarra, M. Nielsen, C.M. Zanetti, $Z_c^+(3900)$ decay width in QCD sum rules, Phys. Rev. D 88 (1) (2013) 016004, https://doi.org/10.1103/PhysRevD.88.016004, arXiv:1304.6433.

[30] P.-Z. Huang, H.-X. Chen, S.-L. Zhu, The strong decay patterns of the 1^{-+} exotic hybrid mesons, Phys. Rev. D 83 (2011) 014021, https://doi.org/10.1103/PhysRevD.83.014021, arXiv:1010.2293.

[31] S.S. Agaev, K. Azizi, H. Sundu, Mass and decay constant of the newly observed exotic $X(5568)$ state, Phys. Rev. D 93 (7) (2016) 074024, https://doi.org/10.1103/PhysRevD.93.074024, arXiv:1602.08642.

[32] S.S. Agaev, K. Azizi, H. Sundu, Strong $Z_c^+(3900) \to J/\psi\pi^+; \eta_c\rho^+$ decays in QCD, Phys. Rev. D 93 (7) (2016) 074002, https://doi.org/10.1103/PhysRevD.93.074002, arXiv:1601.03847.

[33] R.D. Matheus, S. Narison, M. Nielsen, J.M. Richard, Can the X(3872) be a 1++ four-quark state?, Phys. Rev. D 75 (2007) 014005, https://doi.org/10.1103/PhysRevD.75.014005, arXiv:hep-ph/0608297.
[34] P. Colangelo, F. De Fazio, W. Wang, $B_s \to f_0(980)$ form factors and B_s decays into $f_0(980)$, Phys. Rev. D 81 (2010) 074001, https://doi.org/10.1103/PhysRevD.81.074001, arXiv:1002.2880.
[35] P. Ball, V.M. Braun, A. Lenz, Twist-4 distribution amplitudes of the K* and phi mesons in QCD, J. High Energy Phys. 08 (2007) 090, https://doi.org/10.1088/1126-6708/2007/08/090, arXiv:0707.1201.
[36] D.-D. Hu, H.-B. Fu, T. Zhong, Z.-H. Wu, X.-G. Wu, The $a_1(1260)$-meson longitudinal leading-twist distribution amplitude and the semileptonic decays $D \to a_1(1260)\ell^+\nu_\ell$ within the QCD sum rules, arXiv:2107.02758, 2021.
[37] M.A. Olpak, A. Ozpineci, V. Tanriverdi, Light cone distribution amplitudes of excited p-wave heavy quarkonia at leading twist, Phys. Rev. D 96 (1) (2017) 014026, https://doi.org/10.1103/PhysRevD.96.014026, arXiv:1608.04539.
[38] J. Beringer, et al., Review of particle physics, Phys. Rev. D 86 (2012) 010001, https://doi.org/10.1103/PhysRevD.86.010001.
[39] Z.-G. Wang, Q. Xin, Analysis of the pseudoscalar hidden-charm tetraquark states with the QCD sum rules, arXiv:2112.04776, 2021.
[40] Z.-G. Wang, Assignments of the X4140, X4500, X4630, and X4685 based on the QCD sum rules, Adv. High Energy Phys. 2021 (2021) 4426163, https://doi.org/10.1155/2021/4426163, arXiv:2103.04236.
[41] Z.-G. Wang, Z.-Y. Di, Analysis of the mass and width of the $X(4140)$ as axialvector tetraquark state, Eur. Phys. J. C 79 (1) (2019) 72, https://doi.org/10.1140/epjc/s10052-019-6596-8, arXiv:1811.12821.
[42] L. Maiani, F. Piccinini, A.D. Polosa, V. Riquer, The Z(4430) and a new paradigm for spin interactions in tetraquarks, Phys. Rev. D 89 (2014) 114010, https://doi.org/10.1103/PhysRevD.89.114010, arXiv:1405.1551.
[43] M. Nielsen, F.S. Navarra, Charged exotic charmonium states, Mod. Phys. Lett. A 29 (2014) 1430005, https://doi.org/10.1142/S0217732314300055, arXiv:1401.2913.
[44] Z.-G. Wang, Analysis of the $Z(4430)$ as the first radial excitation of the $Z_c(3900)$, Commun. Theor. Phys. 63 (3) (2015) 325–330, https://doi.org/10.1088/0253-6102/63/3/325, arXiv:1405.3581.
[45] R.F. Lebed, A.D. Polosa, $\chi_{c0}(3915)$ as the lightest $c\bar{c}s\bar{s}$ state, Phys. Rev. D 93 (9) (2016) 094024, https://doi.org/10.1103/PhysRevD.93.094024, arXiv:1602.08421.
[46] H.-X. Chen, W. Chen, Settling the Zc(4600) in the charged charmoniumlike family, Phys. Rev. D 99 (7) (2019) 074022, https://doi.org/10.1103/PhysRevD.99.074022, arXiv:1901.06946.
[47] Z.-G. Wang, Axialvector tetraquark candidates for $Z_c(3900)$, $Z_c(4020)$, $Z_c(4430)$, $Z_c(4600)$, Chin. Phys. C 44 (6) (2020) 063105, https://doi.org/10.1088/1674-1137/44/6/063105, arXiv:1901.10741.
[48] M. Ablikim, et al., Precise measurement of the $e^+e^- \to \pi^+\pi^- J/\psi$ cross section at center-of-mass energies from 3.77 to 4.60 GeV, Phys. Rev. Lett. 118 (9) (2017) 092001, https://doi.org/10.1103/PhysRevLett.118.092001, arXiv:1611.01317.
[49] P. Ball, V.M. Braun, The Rho meson light cone distribution amplitudes of leading twist revisited, Phys. Rev. D 54 (1996) 2182–2193, https://doi.org/10.1103/PhysRevD.54.2182, arXiv:hep-ph/9602323.
[50] P. Ball, G.W. Jones, Twist-3 distribution amplitudes of K* and phi mesons, J. High Energy Phys. 03 (2007) 069, https://doi.org/10.1088/1126-6708/2007/03/069, arXiv:hep-ph/0702100.
[51] P. Gubler, A Bayesian Analysis of QCD Sum Rules, Ph.D. thesis, Tokyo Inst. Tech., Tokyo, 2013.